The regulation of enteric neuron connectivity by semaphorin 5A is affected by the autism-associated S956G missense mutation

Morgane E Le Dréan, Catherine Le Berre-Scoul, Vincent Paillé, Martial Caillaud, Thibauld Oullier, Jacques Gonzales, Philippe Hulin, Michel Neunlist, Sophie Talon, Hélène Boudin

iScience

CellPress
OPEN ACCESS

Article

The regulation of enteric neuron connectivity by semaphorin 5A is affected by the autism-associated S956G missense mutation

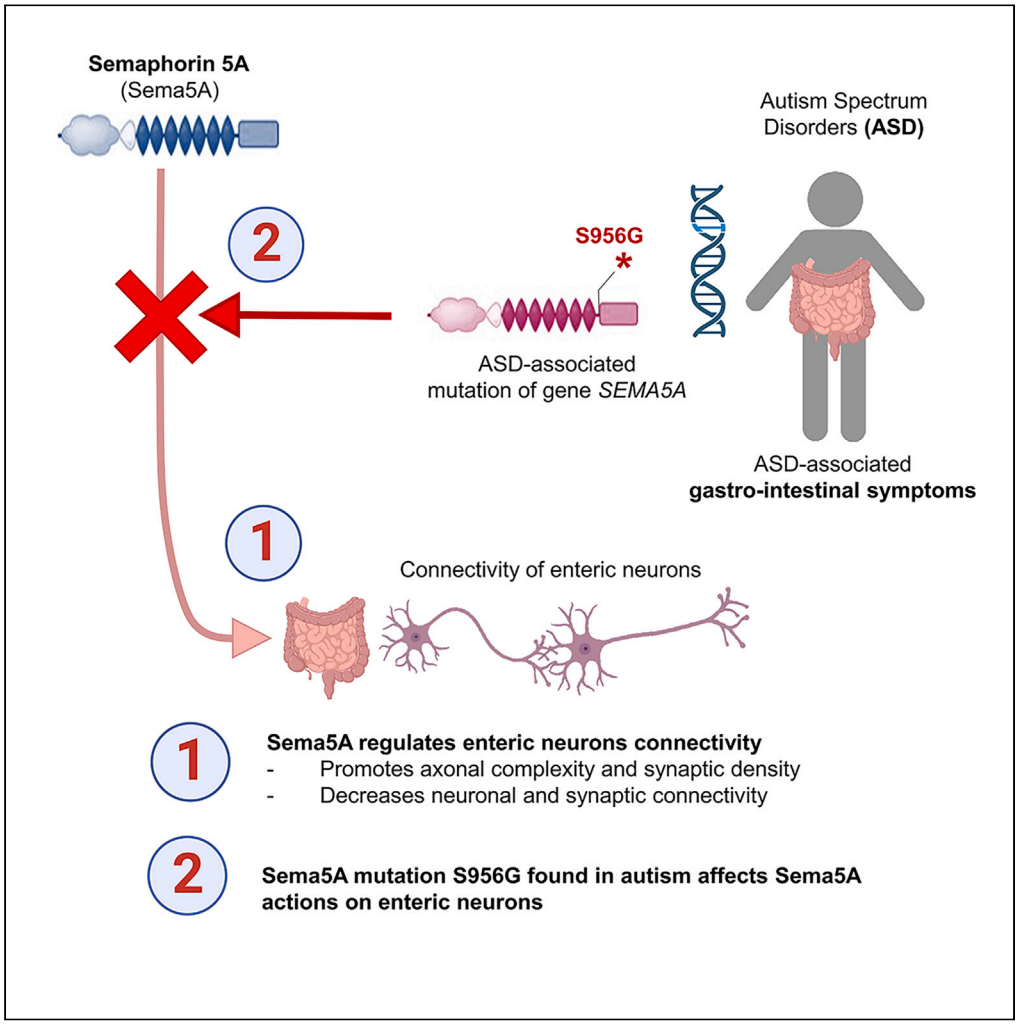

Morgane E. Le Dréan, Catherine Le Berre-Scoul, Vincent Paillé, ..., Michel Neunlist, Sophie Talon, Hélène Boudin

morgane.ledrean@univ-nantes.fr (M.E.L.D.)
helene.boudin@univ-nantes.fr (H.B.)

Highlights

Sema5A and its receptors Plexin A1/A2 are expressed by enteric neurons in rat colon

Sema5A controls synapsin 1 phosphorylation in enteric neurons

Sema5A negatively regulates neuronal activity and synaptic functions

The autism-associated mutation S956G impairs Sema5A activity

Le Dréan et al., iScience 27, 109638
May 17, 2024
https://doi.org/10.1016/j.isci.2024.109638

iScience

CellPress
OPEN ACCESS

Article

The regulation of enteric neuron connectivity by semaphorin 5A is affected by the autism-associated S956G missense mutation

Morgane E. Le Dréan,[1,*] Catherine Le Berre-Scoul,[1,4] Vincent Paillé,[2,4] Martial Caillaud,[1] Thibauld Oullier,[1] Jacques Gonzales,[1] Philippe Hulin,[3] Michel Neunlist,[1] Sophie Talon,[1] and Hélène Boudin[1,5,*]

SUMMARY

The neural network of the enteric nervous system (ENS) underlies gastrointestinal functions. However, the molecular mechanisms involved in enteric neuronal connectivity are poorly characterized. Here, we studied the role of semaphorin 5A (Sema5A), previously characterized in the central nervous system, on ENS neuronal connectivity. Sema5A is linked to autism spectrum disorder (ASD), a neurodevelopmental disorder frequently associated with gastrointestinal comorbidities, and potentially associated with ENS impairments. This study investigated in rat enteric neuron cultures and gut explants the role of Sema5A on enteric neuron connectivity and the impact of ASD-associated mutations on Sema5A activity. Our findings demonstrated that Sema5A promoted axonal complexity and reduced functional connectivity in enteric neurons. Strikingly, the ASD-associated mutation S956G in Sema5A strongly affected these activities. This study identifies a critical role of Sema5A in the ENS as a regulator of neuronal connectivity that might be compromised in ASD.

INTRODUCTION

The enteric nervous system (ENS) consists of an intricate network of neurons and glial cells that regulates gastrointestinal functions.[1] ENS neural network requires not only the assembly of neurons into ganglia but also appropriate growth, orientation, and connectivity of axons and dendrites. The precise mechanisms governing enteric neuronal connectivity as well as molecules involved in these processes remain poorly characterized. However, different classes of molecules, including transcription factors,[2] planar cell polarity pathways,[3] and axonal guidance molecules[4,5] have been shown to regulate ENS connectivity.

Semaphorins are axonal guidance molecules that play a key role in development, maturation, and function of the central nervous system (CNS).[6] Semaphorins are a family of membrane-bound and secreted proteins that are divided, in vertebrates, into five subfamilies from Sema3 to Sema7.[7] Semaphorins signal predominantly through receptor proteins of the plexin and neuropilin families and are implicated in numerous neuronal wiring events in the central and peripheral nervous system,[6,7] but little is known on their potential roles in the regulation of ENS neuronal network in health and disease.

ASD is a neurodevelopmental disorder characterized by deficits in social communication and social interaction, as well as restricted activities and interests. Among the most prevalent comorbidities in ASD are gastrointestinal (GI) symptoms which are 4.4 times more frequent than in neurotypical individuals.[8] The causes of GI symptoms are still unknown but might result from impaired enteric neuronal connectivity, based on the same principle as impaired CNS neuronal connectivity leads to altered behavior. Interestingly, ASD genetic mouse models show gut dysmotility associated with changes in ENS structure, such as the number of enteric neurons, the proportion of neuronal subtypes, and the density of interganglionic fibers.[9–12] Several links have been reported between semaphorin 5A (Sema5A) and ASD. In humans, mutations in the *SEMA5A* gene are associated to severe developmental delays and autism,[13] but the consequences of these mutations on the central and enteric nervous system at cellular levels have never been explored. In addition, mice invalidated for Sema5A exhibit ASD-like behaviors and several brain abnormalities including defects in axonal elongation and synaptic activity.[14,15] Moreover, deletion of Plexin A1 or Plexin A2 receptors, two receptors for Sema5A, alters axonal patterning and synaptogenesis.[16,17] Regarding the gastrointestinal tract, Sema5A deficiency in mice induced increased defecation suggesting the implication of Sema5A in gut functions potentially through modulation of ENS activity.[18]

In this context, Sema5A represents an interesting candidate protein for its potential roles in the regulation of enteric neuron connectivity. However, the expression and the role of Sema5A in the ENS have never been studied. In this study, we aimed to (1) determine the role of

[1]Nantes Université, Inserm, TENS, The Enteric Nervous System in Gut and Brain Diseases, IMAD, Nantes, France
[2]Nantes Université, INRAE, UMR 1280, PhAN, IMAD, 44000 Nantes, France
[3]Plateforme MicroPICell Nantes Université, CHU Nantes, CNRS, INSERM, BioCore, US16, SFR Bonamy, Nantes, France
[4]These authors contributed equally
[5]Lead contact
*Correspondence: morgane.ledrean@univ-nantes.fr (M.E.L.D.), helene.boudin@univ-nantes.fr (H.B.)
https://doi.org/10.1016/j.isci.2024.109638

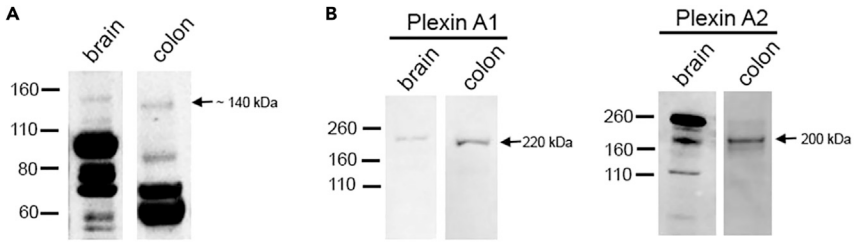

Figure 1. Expression of Sema5A and its receptors Plexin A1 and Plexin A2 in rat brain and colon

(A) Western blot of Sema5A from rat brain and distal colon. For each sample, 10 μg of proteins were loaded on a 4–12% LDS-NuPage and immunoblotted with Sema5A antibody. A band at ~140 kDa was detected as well as additional bands with lower molecular weights.

(B) Western blot of Plexin A1 and Plexin A2 from rat brain and distal colon. In both samples, a band at 220 and 200 kDa was detected for Plexin A1 and Plexin A2, respectively.

Sema5A in axonal patterning and synaptic functions of enteric neurons, and (2) assess the impact of ASD-associated mutations on Sema5A activity. Our findings demonstrated that Sema5A regulated axonal complexity and synaptic functions of enteric neurons. Strikingly, we observed that the ASD-associated S956G mutation in Sema5A strongly affected these activities. This study identifies a critical role of Sema5A in the ENS as a regulator of neuronal connectivity that might be compromised in ASD.

RESULTS

Sema5A and the Plexin A1 and A2 receptors are expressed in enteric neurons of rat distal colon

To first examine whether Sema5A and its receptors Plexin A1/A2 were expressed in the gut, western blots were performed to assess their protein expression in the rat distal colon and brain lysates, the latter being used as a positive control. Regarding Sema5A, we found a band at ~140 kDa in both colon and brain samples with additional bands of lower molecular weights likely resulting from protein degradation or ectodomain shedding as previously described[19–21] (Figure 1A). Regarding the receptors, Plexin A1 and A2 antibodies yielded a band at 220 and 200 kDa respectively in rat brain and colon preparations (Figure 1B). Next, the cellular distribution of Sema5A and Plexin A1/A2 receptors was studied in rat gut. Whole-mount myenteric plexus of distal colons were immunolabeled for Sema5A, Plexin A1, or Plexin A2 in combination with markers of neuronal cell bodies (Hu), axonal fibers (β3-tubulin), and glial cells (S100β). Sema5A immunolabeling was observed in a subset of neuronal cell bodies and processes as shown by respective overlap with Hu and β3-tubulin immunolabeling (Figures 2A, 2A′, 2B, and 2B′). By contrast, Sema5A was not detected in enteric glial cells as shown by a lack of overlap of Sema5A and S100β immunolabeling (Figures 2C, 2C′, 2D, and 2D′). Plexin A1 receptors were observed in axonal fibers and, to a lesser extent, in neuronal cell bodies (Figures 2E and 2E′). Plexin A1 was notably found at the periphery of the neuronal cell bodies suggesting a cell surface localization (Figures 2F and 2F′). Plexin A2 showed an intense immunofluorescence intensity in a subset of neuronal cell bodies corresponding to large neurons and was also observed at the border of small-size enteric neurons and in a few axonal processes (Figures 2G and 2G′). To identify the neurochemical coding of Plexin A2-expressing enteric neurons, immunolabeling was performed for Plexin A2 and markers of cholinergic (choline acetyltransferase, ChAT; Figure 2H), nitrergic (neuronal nitric oxide synthase, nNOS; Figure 2I), and calbindin-expressing neurons (not shown). We found that 49.8 ± 8.4%, 12.4 ± 6.5%, and 16.0 ± 4.1% of total Plexin A2 neurons also express ChAT, nNOS, and calbindin, respectively. Immunolabeling for Plexin A1 and A2 was not found in glial cells (not shown). These results support a selective neuronal expression of Sema5A and the receptors Plexin A1/A2 in the rat distal colon and indicate that the Plexin A2 receptors were mainly expressed by cholinergic neurons.

Sema5A enhances the axonal complexity of enteric neurons, which is abolished by ASD-associated mutation

With the aim of studying the effects of Sema5A on enteric neuronal connectivity using *in vitro* ENS culture models, we first validated the expression of Sema5A and PlexinA1/A2 in a widely used ENS culture model derived from embryonic rat gut.[4,5,22] We found that Sema5A and Plexin A1/A2 were present in neurons, associated with both neuronal cell bodies and axonal processes, but not in glial cells, as observed in rat colon (Figures 3A–3C). These results indicated that the cellular expression and distribution of Sema5A and PlexinA1/A2 in ENS *in vitro* model derived from embryonic rat gut were similar to those in gut tissue.

To study the effects of Sema5A, and its ASD-associated mutations, on the axonal network, several Sema5A plasmid constructs were generated to produce the following recombinant proteins: Sema5A-Fc fusion protein, Sema5A-Fc with the mutation S951C and, S956G, and a control molecule corresponding to the Fc fragment alone. We first verified by western blot that wild-type and mutant Sema5A proteins were successfully expressed and secreted by transfected COS cells in an equivalent amount (supplemental information, Figure S1). To study the impact of Sema5A on the axonal network structure, COS cells transfected with the control Fc or the different Sema5A constructs were suspended in Matrigel, added to ENS cultures, and the resulting cocultures were maintained for 3 days (Figure 4A). Neurons were then immunolabeled for β3-tubulin to reveal the axonal arbor which was analyzed by Sholl analysis, a method previously applied to ENS cultures.[23] Sholl analysis provides measurements of the axonal arbor complexity by integrating axonal length and branches number. Measurements performed in the axonal arbor at a distance of 60 μm from the center of the ganglion showed no difference between the constructs

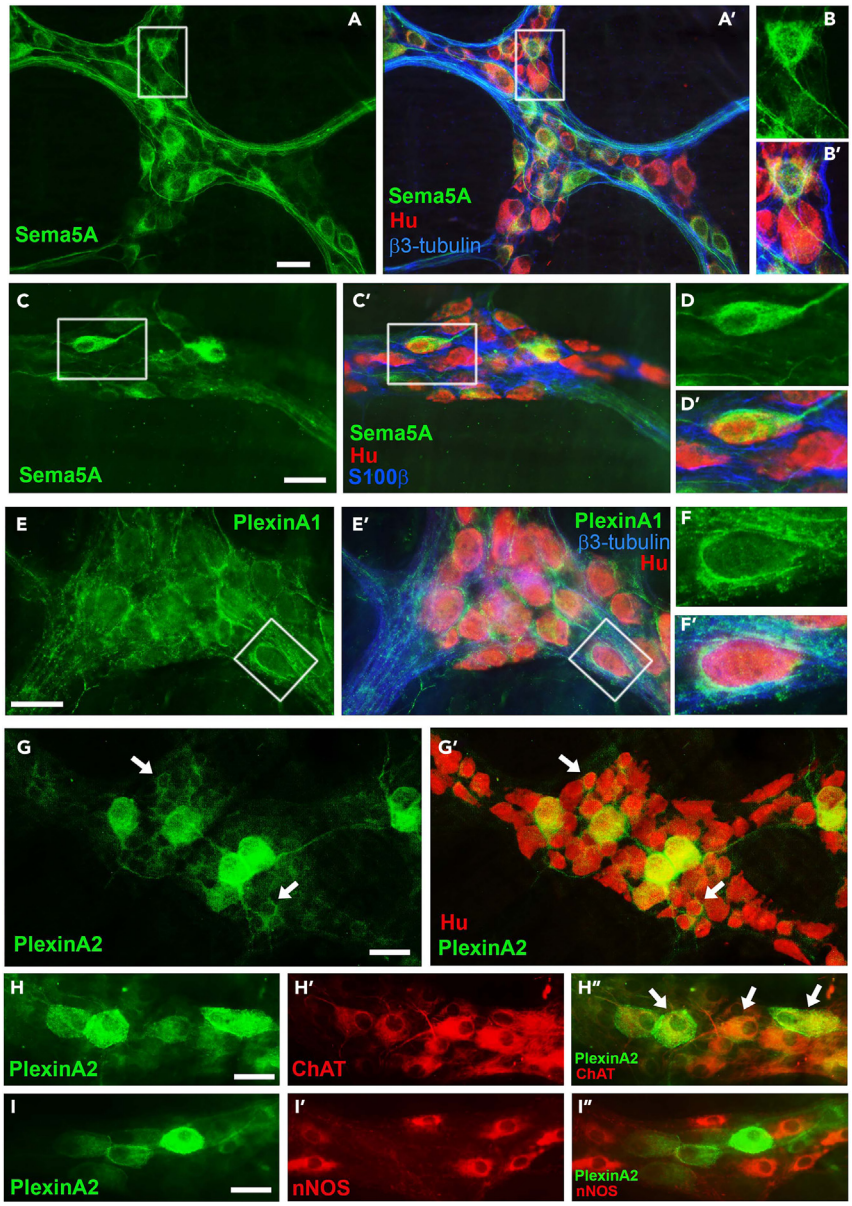

Figure 2. Sema3A and its receptor Plexin A1 and Plexin A2 are expressed in enteric neurons in the rat distal colon

(A, A′, B, and B′) Triple immunolabeling for Sema5A (green), Hu (marker of neuronal soma, red), and β3-tubulin (marker of neuronal soma and axonal processes, blue) in the myenteric plexus of rat distal colon. (B,B′) Higher magnification of the boxed regions in A, A′.

(C, C′, D, and D′) Triple immunolabeling for Sema5A (green), Hu (red), and S100β (marker of glial cells, blue) in the myenteric plexus of rat distal colon. (D, D′) Higher magnification of the boxed regions in C, C′.

(E, E′, F, and F′) Triple immunolabeling for Plexin A1 (green), Hu (red), and β3-tubulin (blue) in the myenteric plexus of rat distal colon. (F, F′) Higher magnification of the boxed regions in E, E′ illustrates the pericellular Plexin A1 labeling.

(G and G′) Double immunolabeling for Plexin A2 (green) and Hu (red) in the myenteric plexus of rat distal colon. The arrows point to small-size enteric neurons showing Plexin A2 at the cell border.

(H, H′, and H″) Double immunolabeling for Plexin A2 (green) and ChAT (red) in the myenteric plexus of rat distal colon. The arrows point to ChAT neurons expressing PlexinA2.

(I, I′, and I″) Double immunolabeling for Plexin A2 (green) and nNOS (red) in the myenteric plexus of rat distal colon. Scale bars, A: 30 μm; C–I: 15 μm.

(Figures 4B and 4C). By contrast, measurements performed in a more distal portion of the axonal arbor (160 μm from the center of the ganglion) showed an increased axonal complexity in the presence of COS cells expressing Sema5A-Fc compared to Fc control condition (n = 6 from 3 independent experiments; p = 0.016, two-way ANOVA with Tukey post-test; Figure 4C). No difference was observed between the

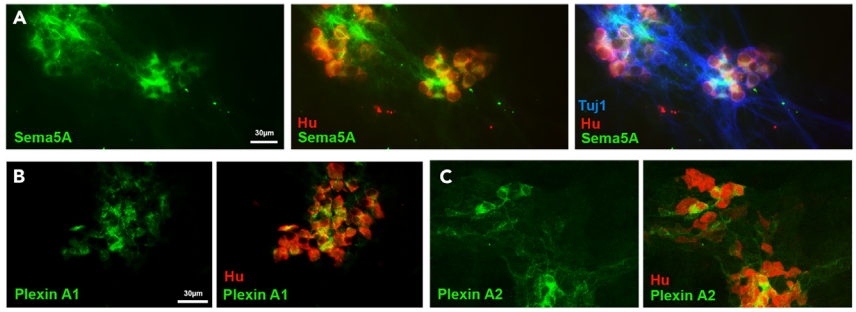

Figure 3. Sema5A, Plexin A1 and Plexin A2 are expressed in enteric neurons in primary cultures of rat gut

(A) Triple immunolabeling for Sema5A (green), Hu (red), and β3-tubulin (blue) at 12 days of culture.

(B) Double labeling of Plexin A1 (green) with Hu (red) at 12 days of culture.

(C) Double labeling of Plexin A2 (green) with Hu (red) at 12 days of culture. Sale bars: 30 µm.

control Fc and the Sema5A mutants, S951C or S956G, at both 60 and 160 µm from the center of the ganglion (Figure 4C). The same results were obtained with the membrane-associated full-length Sema5A (supplemental information Figure S2). Because the extent of axonal arborization also depends on the number of neuronal cell bodies per ganglion, we counted the number of neurons per ganglion and found no difference between groups (n = 7 culture wells from 3 independent experiments; p = 0.256 Kruskal-Wallis; Figure 4D).

Sema5A regulates synapsin 1 clustering and phosphorylation, which is abolished by the ASD-linked S956G mutation

Given that axonal branching and complexity are intricately linked to synapse formation/stabilization,[24] we investigated the impact of Sema5A and its mutant forms on synapses by studying the protein expression and cluster distribution of synapsin 1, a key synaptic protein involved in presynaptic functions. To this aim, we used embryonic rat gut explants, a model previously shown to rapidly develop synapses within 3 days after plating,[5] which is appropriate with the transient expression of Sema5A fusion proteins by COS cells. Embryonic rat gut explants were cocultured for 3 days with transfected COS cells for Fc, Sema5A-Fc or Sema5A-Fc mutant forms placed in Matrigel (Figure 5A). After 3 days of culture, gut explants were collected for western blot analyses or were fixed for immunofluorescence studies. Western blot showed no change in synapsin 1 protein level between groups (Figure 5B), nor in the protein level of the axonal protein β3-tubulin (Figure 5C). To examine whether Sema5A might affect the distribution of synapsin 1 clusters, the number of synapsin 1 clusters was measured on gut explants immunolabeled for β3-tubulin and synapsin 1. Gut explants cultured with Sema5A-Fc-transfected COS cells showed an enhanced density of synaptic clusters compared to explants cultured with Fc-transfected cells (Figures 5D–5F; p = 0.039, ANOVA with Dunn's post-test). While the mutation S951C had no impact on the promoting effect of Sema5A-Fc on synapse density, the mutation S956G inhibited the ability of Sema5A-Fc to enhance synapse density (Figures 5D–5F; p = 0.005, ANOVA with Dunn's post-test). Sema5A-Fc showed no effect on the size of synapsin 1 clusters (Figure 5E). The subcellular localization and function of synapsin 1 is highly regulated by its phosphorylation state. Thus, we examined whether Sema5A might affect synapsin 1 phosphorylation at Ser603, one of the pivotal sites regulating synapsin 1 function and its interaction with synaptic vesicles.[25–27] We found that Sema5A-Fc induced an increased level of phosphorylated synapsin 1 at Ser603 compared to the control Fc condition (supplemental information Figure S3). These results suggest that Sema5A could act on enteric neurons

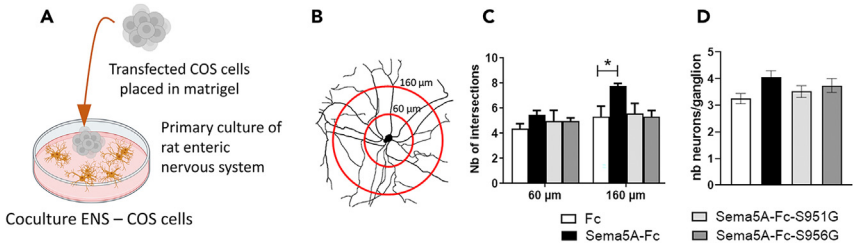

Figure 4. Sema5A stimulates axonal complexity in enteric neurons

(A) Schematic illustrating ENS cocultured with COS cells expressing Fc, Sema5A-Fc, Sema5A-Fc-S951C, or Sema5A-Fc-S956G (See also Figure S1). COS cells suspended in Matrigel were deposited in the center of the ENS culture well and cocultured for 3 days before measuring axonal complexity using Sholl analysis.

(B) Schematic depicting Sholl analysis. Concentric circles were placed at 60 and 160 µm from the ganglion center and the number of axonal intersections with each circle was counted.

(C) Quantification of the number of axonal intersections at 60 and 160 µm from the center of the ganglion. The number of axonal intersections is increased in the presence of Sema5A-Fc as compared to control Fc without affecting the number of neurons per ganglion (D) (See also Figure S2). *p < 0.05, two-way ANOVA with Tukey's post-hoc test; n = 6 culture wells from 3 independent experiments.

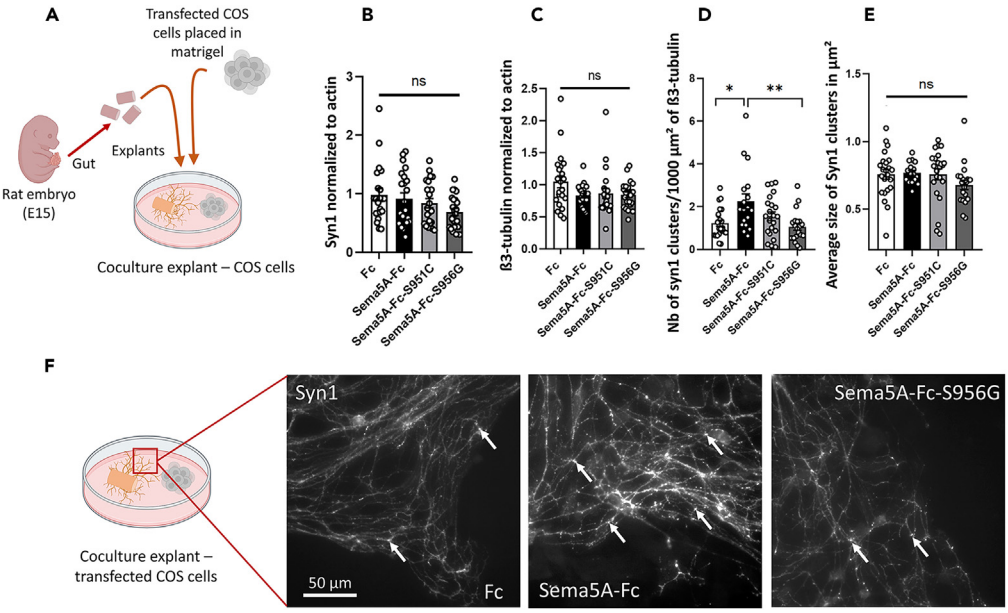

Figure 5. Sema5A enhances the density of synapsin 1 clusters without affecting synapsin 1 protein expression

(A) Schematic illustrating gut explants cocultured with COS cells expressing Fc, Sema5A-Fc, Sema5A-S951C-Fc, or Sema5A-S956G-Fc. Transfected COS cells suspended in Matrigel were deposited in the culture well next to the explant and this coculture was maintained for 3 days. Protein expression was analyzed by western blotting for synapsin 1 (syn1) (B) and the axonal protein β3-tubulin (C). The distribution of synapsin 1 was assessed by immunofluorescence (F) and the number and size of synapsin 1 clusters were measured (D and E). In (F), synapsin 1 clusters are shown by white arrows. (See also Figure S3). Data are mean ± SEM. (western-blot analysis (B and C): n = 22 explants from 4 independent experiments, IHC (D and E) n = 18–23 explants from 6 independent experiments); *$p < 0.05$,**$p < 0.01$, Kruskal-Wallis test, supplemented by Dunn's post-hoc test.

by regulating synapsin 1 clustering and phosphorylation. To further investigate the direct response of enteric neurons to Sema5A stimulation on synapsin 1 phosphorylation, we used a culture model highly purified in enteric neurons.[28] COS cells transfected with Fc, Sema5A-Fc or Sema5A-Fc-S956G constructs were plated on Transwell inserts deposited above enteric neurons to allow the Fc and Sema5A proteins to diffuse from COS cells to enteric neurons. Using site-specific phospho-synapsin 1 antibodies, we analyzed by western blot the levels of synapsin 1 phosphorylation at Ser603 and Ser9, involved in synapsin 1 dissociation from synaptic vesicles,[25,26] and at Ser62/67, involved in synapsin 1 dissociation from actin filaments.[29] We found that Sema5A-Fc, but not the mutant form S956G, induced in enteric neurons an increased level of phosphorylated synapsin 1 at site Ser603 compared to the control Fc condition (Figure 6). The other phosphorylation sites Ser9 and Ser62/67 were unaffected by Sema5A-Fc treatment (Figure 6).

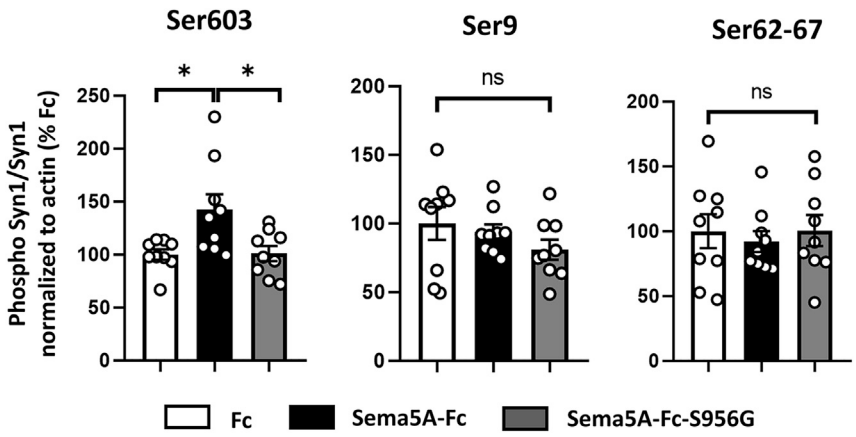

Figure 6. Sema5A increases enteric neurons synapsin 1 phosphorylation at site Ser-603

Western blot analysis of synapsin 1 phosphorylation at site Ser603, Ser9 and Ser62/67 from enteric neuron cultures exposed for 3 days to control Fc, Sema5A-Fc, or Sema5A-S956G-Fc. *$p < 0.05$ Kruskal-Wallis test, supplemented by Dunn's post-hoc test. Data are mean ± SEM, n = 8 cultures from 2 independent experiments.

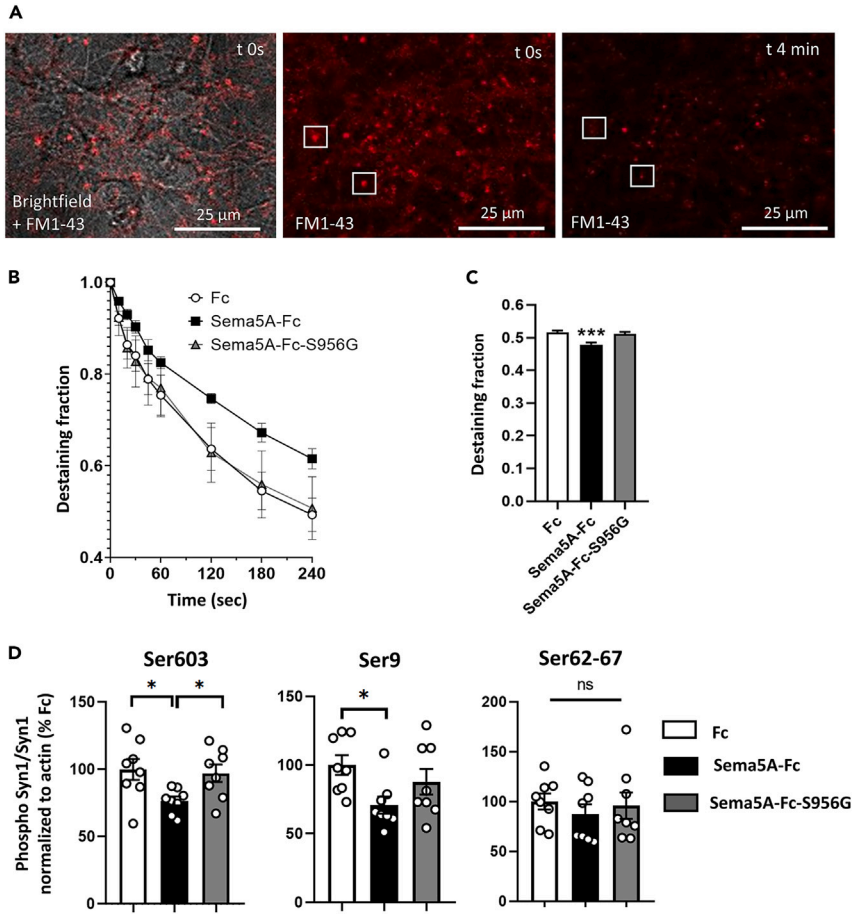

Figure 7. KCl-induced synaptic vesicle exocytosis is reduced by Sema5A in association with a decrease in synapsin 1 phosphorylation at site Ser-603 and Ser-9

(A) From left to right, merged picture of FM1-43 fluorescence and brightfield microscopy at t0s. Representative images of enteric neurons labeled with FM1-43 at t0s and t4 min after 90 mM KCl stimulation.

(B) FM1-43 fluorescence decreases over 4 min exposure to 90 mM KCl.

(C) Remaining fluorescence was measured as destaining fraction, after 4 min exposure to KCl. Destaining fraction of FM1-43 fluorescence is expressed as 1-(Fluo t4 min/Fluo at t0). Data are mean ± SEM. ($n = 60$ clusters per culture well, from 12 culture wells from 4 independent experiments); ***$p < 0.001$, One-way ANOVA with Tukey's multiple comparisons test.

(D) Neurons were depolarized by 1 min exposure to 90 mM KCl and collected for western blot analysis and assessment of synapsin 1 phosphorylation at site Ser-603, Ser-9 and Ser-62/67. *$p < 0.05$ Kruskal-Wallis test, supplemented by Dunn's post-hoc test. Data are mean ± SEM, $n = 8$ cultures from 2 independent experiments.

Sema5A decreases synaptic vesicle exocytosis and the ASD-linked S956G mutation abrogates these effects

Phosphorylation of synapsin 1 at Ser603 acts as a molecular trigger, leading to the dissociation of synapsin 1 from synaptic vesicles. This mechanism plays a crucial role in synaptic vesicle release at the active zone.[25–27] Thus, we investigated the impact of Sema5A on synaptic vesicle exocytosis by imaging the presynaptic release of the dye FM1-43 as previously described in central and enteric neurons.[28,30,31] After FM1-43 loading in neurons within synaptic vesicles, enteric neurons were stimulated by KCl-induced depolarization for 4 min and the fluorescence decrease was recorded. The decrease of FM1-43 fluorescence intensity corresponds to the fusion of synaptic vesicles with the plasma membrane and the release of the dye, therefore providing an indicator of the synaptic vesicle exocytosis activity (Figure 7A). Measurements of the fluorescence intensity of FM1-43 clusters over the 4 min of recording showed that the loss of fluorescence was reduced when enteric neurons were cocultured with COS cells transfected with Sema5A-Fc compared to control Fc or the mutant Sema5A-Fc-S956G (Figure 7B). Quantification performed at 4 min after the addition of KCl indicated that the destaining fraction was significantly lower in the presence of Sema5A-Fc than control Fc or the mutant Sema5A-Fc-S956G suggesting that Sema5A reduced synaptic vesicle release induced by KCl depolarization and lost this activity with the S956G mutation (Figure 7C). In parallel, we examined the effects of Sema5A-Fc on synapsin 1 phosphorylation upon neuronal depolarization induced by KCl. Sema5A-Fc induced a reduced phosphorylation level at Ser603 and Ser9 compared to neurons cocultured with COS cells expressing the control Fc (Figure 7D). Moreover, the reduced level of synapsin 1 phosphorylation at Ser603 was not

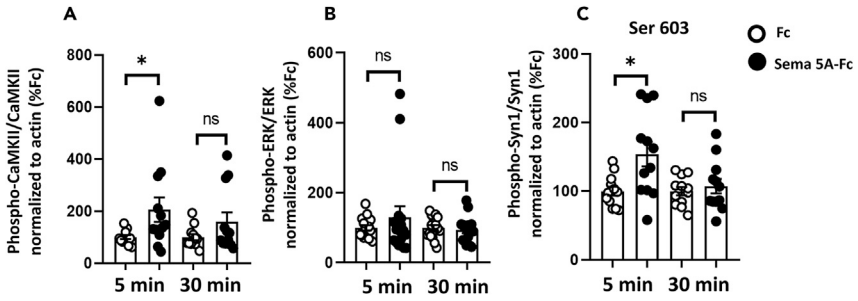

Figure 8. Enteric neurons exposed to Sema5A for 5 min show increased CaMKII phosphorylation and synapsin 1 phosphorylation at site Ser603

Enteric neurons were treated for 5 min or 30 min with Fc fragment or Sema5A-Fc (4.5 μM). Western blot for phosphorylated CaMKII at Tyr286 (A), phosphorylated ERK at Thr202/Tyr204 (B), and synapsin 1 at Ser-603 (C). *$p < 0.05$ Mann-Whitney test for each time group. Data are mean ± SEM, $n = 12$ to 16 cultures from 3 to 4 independent experiments.

observed in neurons cocultured with COS cells expressing Sema5A-Fc-S956G (Figure 7D). No change for the phosphorylation site Ser62/67 was observed between groups (Figure 7D). Previous studies indicate that Ser603 and Ser9 are phosphorylated by Ca^{2+}/calmodulin-dependent protein kinase II (CaMKII) and CaMKII/protein kinase A respectively while Ser62/67 is phosphorylated by extracellular signal-regulated kinase (ERK).[25,29] Therefore, we asked whether Sema5A could induce CaMKII or ERK activation by examining their level of phosphorylation at Tyr286 and Thr202/Tyr204, respectively. Enteric neurons exposed to Sema5A for 5 min showed an increased CaMKII phosphorylation while ERK phosphorylation was unaffected (Figures 8A and 8B). In addition, the Sema5A-induced increase in CaMKII phosphorylation was associated with an increased level of synapsin 1 phosphorylation at Ser603 (Figure 8C). Altogether, these results suggest that Sema5A modulates synapsin 1 phosphorylation potentially through the activation of CaMKII.

Sema5A reduces activity and connectivity of enteric neurons

To investigate whether the effects induced by Sema5A on synaptic vesicle exocytosis and synapsin phosphorylation could translate into changes in the electrophysiological properties of enteric neurons, cell-attached and whole-cell patch-clamp recordings were performed as previously established.[28] In the cell-attached configuration, we observed several changes induced by Sema5A-Fc exposure compared to control Fc, including a decreased number of spontaneously firing neurons (56% vs. 33% of total neurons upon Fc and Sema5A-Fc exposure, respectively; Figure 9B). Moreover, among these spontaneously active neurons (Fc $n = 9$ and Sema5A-Fc $n = 5$), we observed a marked reduction (5-fold) in firing frequency upon exposure to Sema5A compared to control conditions (Figures 9A–9C). These findings suggest that Sema5A regulates the functional properties of enteric neurons, through the potential modulation of their electrophysiological characteristics. In the whole-cell configuration, we conducted measurements of passive and active membrane properties in neurons treated with Sema5A and control-treated neurons (Table 1). Our observations revealed a significant decrease in the action potential (AP) amplitude in Sema5A-Fc condition (Table 1) as determined through voltage response measurements upon 30 pA current pulses as illustrated in Figure 9E. Of note, the steady-state average I/V relationship was unaffected by Sema5A-Fc exposure (Table 1; Figure 9D). Subsequently, we explored miniature postsynaptic currents (mPSCs) to assess synaptic spontaneous activity (minis recordings). Neurons exposed to Sema5A ($n = 12$) exhibited a more than 3-fold significant reduction in mPSC frequency compared to the control condition ($n = 11$) (Figures 9F and 9G). However, Sema5A-exposed neurons displayed normal amplitude (Figure 9H), rise time (Figure 9I), and duration (Figure 9J) of mPSCs. These results provide additional evidence supporting the negative regulatory role of Sema5A on neuronal activity and connectivity.

DISCUSSION

In this study, we provide evidence that Sema5A, encoded by the *SEMA5A* susceptibility gene for autism, is expressed by enteric neurons and regulates their functional connectivity. Our data showed that Sema5A increases the axonal complexity and synapse density of enteric neurons. At the synaptic level, Sema5A reduces synaptic vesicle exocytosis and controls synapsin 1 phosphorylation. Furthermore, Sema5A negatively regulates the spontaneous activity and the frequency of miniature post-synaptic currents of enteric neurons. Remarkably, the ASD-linked S956G mutation affects Sema5A activity. This study identifies a critical role of Sema5A in the ENS as a regulator of neuronal activity and connectivity that might be compromised by ASD-associated mutations.

First, we showed that Sema5A and its related receptors Plexin A1 and Plexin A2 were selectively expressed by enteric neurons in rat colon. Western blot analysis for Sema5A showed a band at 140 kDa in brain and gut-derived samples, consistent with the reported molecular weight in various tissues and cell lines.[19,20,32,33] We also observed Sema5A-immunoreactive bands at molecular weights lower than 140 kDa, notably in the range of 90–110 kDa, corresponding to the molecular weight of a soluble form of Sema5A resulting from proteolytic cleavage of the extracellular domain shown to be released by various cell lines.[21,34] Therefore, the 90–110 kDa forms detected in brain and colon might represent a secreted form of Sema5A. At the cellular level in rat colon and ENS cultures, Sema5A, Plexin A1 and A2 receptors were selectively expressed by enteric neurons but not by enteric glial cells. The identity of the receptors mediating Sema5A activity in enteric neurons has not

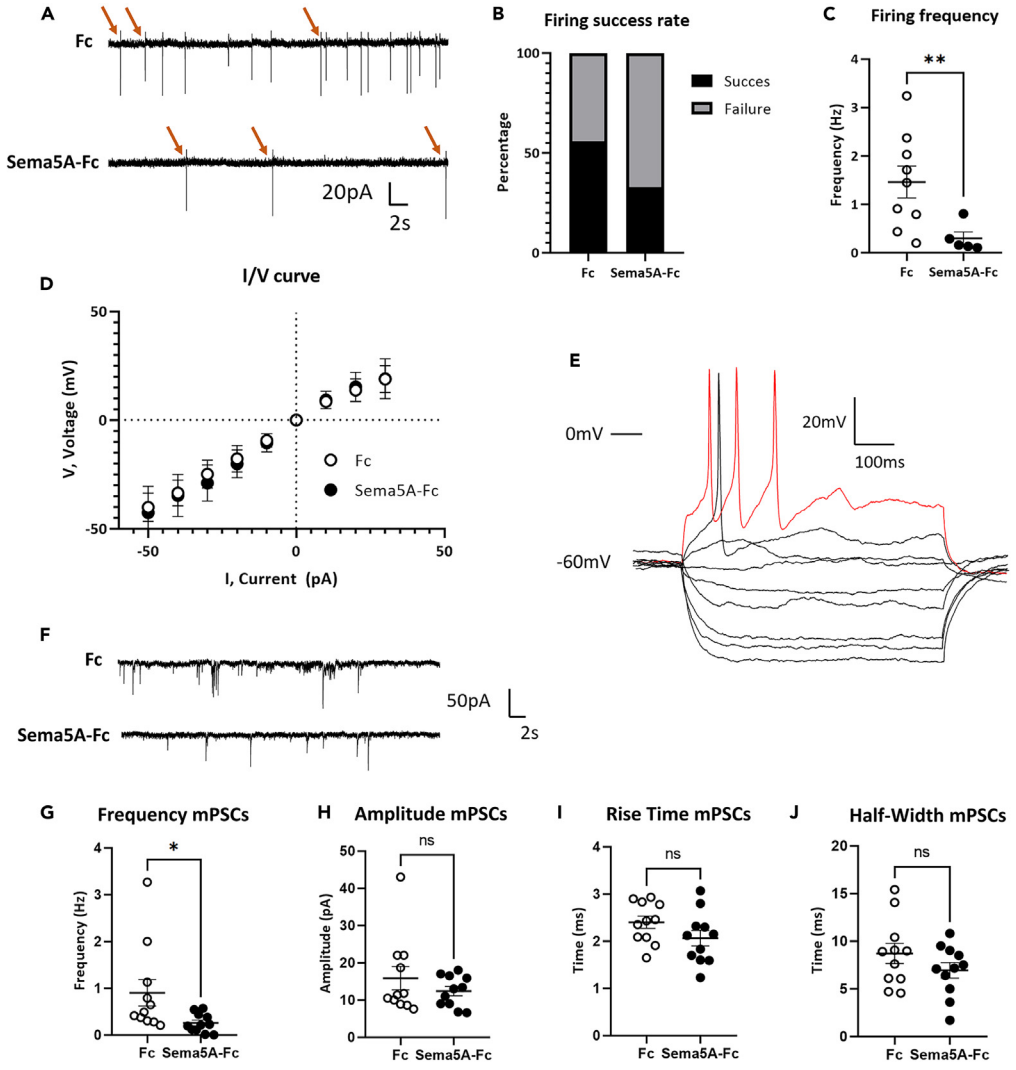

Figure 9. Sema5A impacts connectivity and synaptic properties in enteric neurons

Electrophysiological properties of enteric neurons cocultured for 3 days with COS cells expressing Fc or Sema5A-Fc, were measured in the cell-attached and whole-cell configuration.

(A and C) Cell-attached configuration. (A) Representative traces of enteric neuron spontaneous activity in Fc or Sema5A-Fc condition. Red arrows highlight spontaneous spikes.

(B and C) Sema5A-Fc exposure reduces the number of spontaneously active neurons (B) and the firing frequency of active neurons (C).

(D and E) Exploration of the passive and active membrane properties of primary enteric neurons measured in whole-cell configuration. (D) Steady-state average I/V relationship from enteric neurons.

(E) Raw traces depicting individual voltage responses to a series of 500 ms current pulses ranging from −50 pA to +20 pA in 10 pA steps, and to +30 pA above the rheobase (red trace). Passive and active membrane properties of enteric neurons recorded in the current-clamp configuration are summarized in Table 1.

(F) Representative traces of miniature postsynaptic currents (mPSCs) recorded in whole-cell configuration from enteric neurons exposed to Fc or Sema5A-Fc. Quantitative analysis of mPSC frequency (G), amplitude (H), rise time (I), and half-width duration (J) reveal a significant difference in mPSC frequency between the Fc and Sema5A conditions. Mann-Whitney test $*p < 0.05$. Data are mean ± SEM, with at least $n = 10$ neurons per condition (except spontaneous firing Fc $n = 9$ and Sema5A-Fc $n = 5$) from 3 independent experiments.

been addressed in this study. Both Plexin A1 and Plexin A2 represent attractive candidate receptors giving their cellular distribution in enteric neurons and their reported involvement in Sema5A signaling in other contexts including central neurons and cancer cell lines.[6,14] Interestingly, we found that Plexin A2 receptors were mainly expressed by cholinergic neurons suggesting that binding of Sema5A to Plexin A2 might preferentially modulate the function of cholinergic neurons. Another plexin receptor, Plexin D1, has been reported to be involved in the regulation of ChAT expression in motor neurons.[35] Whether Sema5A/Plexin A2 interaction might also regulate ChAT expression and, therefore, impact on cholinergic neurotransmission remains to be determined.

Table 1. Summary of passive and active membrane properties of enteric neurons recorded in the whole-cell configuration

	No. of cells	Ri steady state (Mo)	Rheobase (pA)	AP Frequency (Hz) +30pA	AP amplitude (mV)	AP duration (ms)	AP rise time (ms)	AP decay time (ms)
Fc	10	867,3 ± 57,09	27,5 ± 2,814	5 ± 1,011	54,41 ± 1,87	10,45 ± 1,271	5,08 ± 0,7657	5,371 ± 0.614
Sema5A-Fc	12	973,3 ± 41,44	25,42 ± 4,458	5,833 ± 1,381	43,87 ± 2,002	11,18 ± 0,8418	5,857 ± 0,6378	5,233 ± 0,4715
	p-value	0,1403	0,7103	0,8759	0,0011	0,6266	0,4409	0,8588

The patterning of axonal arbor and synaptic connections underlie neuronal connectivity that drives coordinated functions of the ENS. In this study, we identified Sema5A as a molecular signal controlling these processes by promoting axonal complexity and limiting synaptic activity. The methodology used to assess the extent of axonal arbor was based on Sholl analysis, which integrates both the length and the number of axonal fibers. The fact that a facilitating effect was observed at a distance, but not close, from the ganglion suggests that Sema5A would mostly regulate terminal arborization but not the number of primary axons emerging from neuronal cell bodies. This interpretation is supported by protein expression level of the axonal protein β3-tubulin, unaffected by Sema5A stimulation. These results suggest that the main axonal fibers were preserved but that Sema5A would regulate fine distal axonal branching, containing a low level of β3-tubulin, therefore marginally contributing to the total amount of β3-tubulin. The Sema5A-induced promoting effect on axonal arbor extension of enteric neurons is consistent with previous studies reporting a permissive activity of Sema5A on axon elongation of dorsal root ganglia and in the diencephalon.[15,20] The Sema5A-induced effects in the distal region of the axonal arborization could have consequences on the maturation of ENS functional network. The terminal part of the axonal arbor contains numerous branches emanating from the axon shaft. These terminal branches are engaged in making connections with specific targets that eventually stabilize into functional synapses.[36] Sema5A could therefore regulate the first stages involved in the formation of synaptic contacts. Axonal arbor shaping could also impact gut functions, in particular gut motility. It has been shown that distinct axonal projection lengths and orientations in the mouse colon were correlated to specific motility patterns.[37] Furthermore, disruption of the axonal tract configuration is associated with bowel dysmotility.[3] Therefore, the establishment and maintenance of the axonal arbor of enteric neurons are crucial mechanisms underlying gut motility. Mutant mice expressing a truncated form of Sema5A exhibit increased defecation,[18] suggesting the involvement of Sema5A in the regulation of gut motility. We propose that the role of Sema5A in controlling distal axonal extensions could contribute to the maturation of enteric neuron axonal network and consequently to gastrointestinal motility.

In addition, we found that Sema5A increased the number of synapses, defined as synapsin 1 clusters, and the level of synapsin 1 phosphorylation at Ser603. Phosphorylation at Ser603 represents a molecular signal for synapsin 1 dissociation from synaptic vesicles, resulting in dispersion of synapsin 1 from presynaptic terminals to axonal regions.[25] It is thus expected that an increased synaptic clustering of synapsin 1 would be associated with a decreased level of Ser603 phosphorylation, which is not the case in our study. It is therefore unlikely that the mechanism underlying the Sema5A-induced clustering of synapsin 1 relies on the ability of Sema5A to increase the synapsin 1 phosphorylation level at Ser603. The presynaptic targeting of synapsin 1 has been shown to be regulated by *O*-glycosylation at several Ser residues[38] and by multiple molecular interactions between different domains constituting synapsin 1 and between synapsin 1 isoforms.[39] Whether Sema5A-induced synapsin 1 clustering in enteric neurons is achieved through regulation of *O*-glycosylation or homo- and heterodimerization of synapsin 1 remains to be studied.

Interestingly, we found that Sema5A exerts a bidirectional control of synapsin 1 phosphorylation depending on neuronal depolarization. Under resting condition, Sema5A increased phosphorylation at Ser603 while no modification of phosphorylation was observed at Ser9 and Ser62/67. The phosphorylation at Ser603 and Ser9, achieved by Ca^{2+}/calmodulin-dependent protein kinase II (CaMKII) and CaMKII/protein kinase A respectively, promotes the dissociation of synapsin 1 from synaptic vesicles, resulting in the transition of the synaptic vesicles from a reserve pool to a readily releasable pool as a mechanism enabling sustained synaptic transmission.[40] Phosphorylation at Ser62/67, achieved by ERK, reduces the interaction between synapsin 1 and actin cytoskeleton contributing also to the docking of synaptic vesicles in the readily releasable pool.[29] By showing a selective increase of Ser603 phosphorylation induced by Sema5A, compared to Ser9 and Ser62/67, our data suggest that Sema5A would preferentially decrease tethering of synapsin 1 to synaptic vesicles through CaMKII activation. In agreement with this hypothesis, we found that Sema5A increased the phosphorylation of CaMKII at Tyr-286, but not that of ERK. Another possibility is that Sema5A could inhibit the activity of the protein phosphatase A2 shown to be involved in the dephosphorylation of synapsin 1 at Ser603.[41] Upon neuronal depolarization, pretreatment of enteric neurons with Sema5A reduced the phosphorylation at Ser603 and Ser9 compared to neurons pretreated with Fc. It is well-established that depolarization-driven phospho-signaling targets several phosphorylation sites on synapsin 1 that promote the availability of synaptic vesicles at the active zone for exocytosis. By showing that Sema5A inhibits synapsin 1 phosphorylation at Ser603 and Ser9 upon neuronal depolarization, our results suggest an inhibitory role of Sema5A on synaptic vesicle exocytosis. Accordingly, we found by FM1-43 imaging that Sema5A reduces synaptic vesicle release induced by KCl depolarization. Therefore, one can hypothesize that upon neuronal depolarization, Sema5A negatively regulates synaptic vesicle exocytosis through the inhibition of synapsin 1 phosphorylation at Ser603 and Ser9. Altogether, our results identify Sema5A as a bifunctional regulator of synapsin 1 phosphorylation in an activity-dependent manner. Under resting conditions, by facilitating synapsin 1 phosphorylation at Ser603, Sema5A would promote the translocation of synaptic vesicles to the readily releasing pool, while upon neuronal depolarization, Sema5A would reduce synapsin 1 phosphorylation at Ser603 and Ser9, thus restraining synaptic vesicle exocytosis. The ability of Sema5A to exert bifunctional activity depending on the

environmental context aligns with previous studies in the central nervous system, showing that Sema5A can exhibit facilitating or inhibitory activity on axonal guidance according to the molecular composition of the extracellular matrix.[20] Whether this dual activity of Sema5A also relies on its molecular form as a membrane-bound or secreted proteolytic-cleaved protein, as shown for Sema5B in synapse elimination[42] remains to be determined.

We further demonstrated by patch-clamp experiments that Sema5A exerted a functional impact on enteric neurons. Specifically, Sema5A significantly influenced both the occurrence and frequency of spontaneous firing. While Sema5A had mild effects on passive and active membrane properties, it markedly decreased the frequency (though not amplitude) of miniature postsynaptic currents (mPSCs). This reduction in mPSC frequency and firing frequency may indicate a synaptic disorganization, potentially attributable to two key mechanisms: (1) presynaptic alterations involving decreased neuronal connectivity and a diminished probability of neurotransmitter release, and (2) post-synaptic modifications, potentially leading to a complete reorganization of protein assemblies forming postsynaptic densities. Our results showing that Sema5A reduced synaptic vesicle release would favor the involvement of a presynaptic mechanism in the Sema5A-induced decrease of mPSCs. This inhibitory activity of Sema5A on synaptic activity is consistent with previous studies showing that the knockdown of Sema5A increased miniature excitatory post-synaptic currents (mEPSC) frequency and amplitude in the hippocampus, indicating an inhibitory activity of Sema5A on brain synaptic transmission.[14] This shared activity of Sema5A between the gut and the brain supports the existence of gut-brain molecular interaction.

We also investigated the impact of a Sema5A ASD-associated mutation (S956G) on Sema5A enteric neuron connectivity and presynaptic activity. We observed that this mutation abolished Sema5A-induced effects on axonal arborization, synapsin 1 cluster density and synaptic vesicle release. The mutation S956G is a missense variant affecting a conserved amino acid located just before the first thrombospondin domain.[13] The thrombospondin repeats of Sema5A have been shown to play a critical role in the interaction with the extracellular matrix, influencing Sema5A activity on central neuron connectivity.[20] Therefore, the S956G mutation could limit Sema5A's ability to interact with component of the extracellular matrix or other binding partners yet to be characterized. The S951C mutation located in the same Sema5A molecular domain as the S956G mutation preserved Sema5A activity. This result is unclear but suggests that this mutation likely maintains the molecular conformation of Sema5A required to exert its activity on the studied parameters. The loss of function of Sema5A induced by the S956G mutation on its inhibitory activity on synaptic vesicle exocytosis suggests that impaired synaptic vesicle dynamics of enteric neurons could be associated with autism. In agreement with this, mutations found in synapsin 1 and associated with ASD induce defects in synaptic vesicle availability or exocytosis.[43,44] By showing that Sema5A-associated ASD mutation disrupted Sema5A activity on synapsin 1 phosphorylation and synaptic vesicle dynamic, our study supports the importance of impaired presynaptic mechanisms in ASD. Previous studies have shown that mice expressing a Sema5A deletion mutant defecate more than wildtype mice,[18] suggesting that deficiency in Sema5A affects gut motility. We propose that the deficiency of Sema5A generated by the ASD-associated S956G mutation could contribute to gut motility disorders due to impaired Sema5A activity in regulating enteric neuron networks and/or connectivity.

In conclusion, this study sheds light on the role of Sema5A in enteric neuron connectivity and synaptic functions and demonstrates the impact of an ASD-associated mutation on Sema5A activity that might potentially contribute to ENS dysfunctions and, therefore, gastrointestinal symptoms in ASD.

Limitations of the study

One limitation of this study is the lack of *in vivo* evidence that Sema5A regulates enteric neuron connectivity. The examination of the enteric neuron network in the gut of Sema5A$^{-/-}$ mice in future studies would enhance the physiological robustness of our findings. Furthermore, although we identified a previously undescribed significance of the ASD-associated Sema5A mutation S956G on Sema5A activity, the validation of these findings in *in vivo* models would require the future availability of transgenic mouse lines that specifically express this Sema5A mutant form in enteric neurons.

STAR★METHODS

Detailed methods are provided in the online version of this paper and include the following:

- KEY RESOURCES TABLE
- RESOURCE AVAILABILITY
  - Lead contact
  - Materials availability
  - Data and code availability
- EXPERIMENTAL MODEL AND STUDY PARTICIPANT DETAILS
  - Animals
  - Cells
- METHOD DETAILS
  - Western blot
  - Immunofluorescence staining
  - Plasmid constructs
  - Cell cultures

- Sema5A acute treatment on enteric neurons cultures
- FM1-43 imaging
- Patch clamp electrophysiology
- Whole-cell patch clamp

- QUANTIFICATION AND STATISTICAL ANALYSIS

SUPPLEMENTAL INFORMATION

Supplemental information can be found online at https://doi.org/10.1016/j.isci.2024.109638.

ACKNOWLEDGMENTS

The expression vectors encoding Fc and Sema5A-Fc were a gift from AL. Kolodkin (Johns Hopkins University). We thank P. Bréhéret for initial experiments. The 6G7 anti β3-tubulin antibody developed by University of Pittsburgh was obtained from the Developmental Studies Hybridoma Bank, created by the NICHD of the NIH and maintained at The University of Iowa, Department of Biology, Iowa City, IA 52242. This work was supported by Inserm, INRAE, Région Pays de la Loire (Enterautisme), ANR Microbiautism (ANR-10-INBS-04), ExtraNeuro (ANR-22-CE14-0043), and Ministère de l'Enseignement Supérieur et de la Recherche (PhD fellowship to MELD). We acknowledge the IBISA MicroPICell facility (Biogenouest), member of the national infrastructure France-Bioimaging supported by the French National Research Agency (ANR-10-INBS-04).

AUTHOR CONTRIBUTIONS

M.E.L.D., S.T., V.P., and H.B. designed the study; M.E.L.D., C.L.B.S., M.C., T.O., and J.G. performed the experiments; P.H. helped for confocal microscopy and image analyses; M.E.L.D., C.L.B.S., V.P., S.T., and H.B. analyzed data and interpreted results; M.E.L.D., V.P., and H.B. wrote the manuscript and prepared figures; M.E.L.D. and H.B. supervised the project; M.C. and M.N. revised the manuscript. All authors read and approved the final manuscript.

DECLARATION OF INTERESTS

The authors declare no competing interests.

Received: July 29, 2023
Revised: February 29, 2024
Accepted: March 26, 2024
Published: March 28, 2024

REFERENCES

1. Furness, J.B. (2012). The enteric nervous system and neurogastroenterology. Nat. Rev. Gastroenterol. Hepatol. *9*, 286–294. https://doi.org/10.1038/nrgastro.2012.32.
2. Chalazonitis, A., Tang, A.A., Shang, Y., Pham, T.D., Hsieh, I., Setlik, W., Gershon, M.D., and Huang, E.J. (2011). Homeodomain interacting protein kinase 2 regulates postnatal development of enteric dopaminergic neurons and glia via BMP signaling. J. Neurosci. *31*, 13746–13757. https://doi.org/10.1523/JNEUROSCI.1078-11.2011.
3. Sasselli, V., Boesmans, W., Vanden Berghe, P., Tissir, F., Goffinet, A.M., and Pachnis, V. (2013). Planar cell polarity genes control the connectivity of enteric neurons. J. Clin. Invest. *123*, 1763–1772. https://doi.org/10.1172/JCI66759.
4. Bodin, R., Paillé, V., Oullier, T., Durand, T., Aubert, P., Le Berre-Scoul, C., Hulin, P., Neunlist, M., and Cissé, M. (2021). The ephrin receptor EphB2 regulates the connectivity and activity of enteric neurons. J. Biol. Chem. *297*, 101300. https://doi.org/10.1016/j.jbc.2021.101300.
5. Gonzales, J., Le Berre-Scoul, C., Dariel, A., Bréhéret, P., Neunlist, M., and Boudin, H. (2020). Semaphorin 3A controls enteric neuron connectivity and is inversely associated with synapsin 1 expression in Hirschsprung disease. Sci. Rep. *10*, 15119. https://doi.org/10.1038/s41598-020-71865-3.
6. Pasterkamp, R.J. (2012). Getting neural circuits into shape with semaphorins. Nat. Rev. Neurosci. *13*, 605–618. https://doi.org/10.1038/nrn3302.
7. Mizuno, Y., Nakanishi, Y., and Kumanogoh, A. (2023). Pathophysiological functions of semaphorins in the sympathetic nervous system. Inflamm. Regen. *43*, 30. https://doi.org/10.1186/s41232-023-00281-7.
8. McElhanon, B.O., McCracken, C., Karpen, S., and Sharp, W.G. (2014). Gastrointestinal symptoms in autism spectrum disorder: a meta-analysis. Pediatrics *133*, 872–883. https://doi.org/10.1542/peds.2013-3995.
9. Bernier, R., Golzio, C., Xiong, B., Stessman, H.A., Coe, B.P., Penn, O., Witherspoon, K., Gerdts, J., Baker, C., Vulto-van Silfhout, A.T., et al. (2014). Disruptive CHD8 mutations define a subtype of autism early in development. Cell *158*, 263–276. https://doi.org/10.1016/j.cell.2014.06.017.
10. Golubeva, A.V., Joyce, S.A., Moloney, G., Burokas, A., Sherwin, E., Arboleya, S., Flynn, I., Khochanskiy, D., Moya-Pérez, A., Peterson, V., et al. (2017). Microbiota-related Changes in Bile Acid & Tryptophan Metabolism are Associated with Gastrointestinal Dysfunction in a Mouse Model of Autism. EBioMedicine *24*, 166–178. https://doi.org/10.1016/j.ebiom.2017.09.020.
11. Hosie, S., Ellis, M., Swaminathan, M., Ramalhosa, F., Seger, G.O., Balasuriya, G.K., Gillberg, C., Råstam, M., Churilov, L., McKeown, S.J., et al. (2019). Gastrointestinal dysfunction in patients and mice expressing the autism-associated R451C mutation in neuroligin-3. Autism Res. *12*, 1043–1056. https://doi.org/10.1002/aur.2127.
12. Margolis, K.G., Li, Z., Stevanovic, K., Saurman, V., Israelyan, N., Anderson, G.M., Snyder, I., Veenstra-VanderWeele, J., Blakely, R.D., and Gershon, M.D. (2016). Serotonin transporter variant drives preventable gastrointestinal abnormalities in development and function. J. Clin. Invest. *126*, 2221–2235. https://doi.org/10.1172/JCI84877.
13. Mosca-Boidron, A.L., Gueneau, L., Huguet, G., Goldenberg, A., Henry, C., Gigot, N., Pallesi-Pocachard, E., Falace, A., Duplomb, L., Thevenon, J., et al. (2016). A de novo microdeletion of SEMA5A in a boy with autism spectrum disorder and intellectual disability. Eur. J. Hum. Genet. *24*, 838–843. https://doi.org/10.1038/ejhg.2015.211.
14. Duan, Y., Wang, S.H., Song, J., Mironova, Y., Ming, G.L., Kolodkin, A.L., and Giger, R.J. (2014). Semaphorin 5A inhibits

synaptogenesis in early postnatal- and adult-born hippocampal dentate granule cells. Elife *3*, e04390. https://doi.org/10.7554/eLife.04390.

15. Masuda, T., Sakuma, C., Yaginuma, H., and Taniguchi, M. (2014). Attractive and permissive activities of semaphorin 5A toward dorsal root ganglion axons in higher vertebrate embryos. Cell Adh. Migr. *8*, 603–606. https://doi.org/10.4161/19336918.2014.972770.
16. Zhao, X.F., Kohen, R., Parent, R., Duan, Y., Fisher, G.L., Korn, M.J., Ji, L., Wan, G., Jin, J., Püschel, A.W., et al. (2018). PlexinA2 Forward Signaling through Rap1 GTPases Regulates Dentate Gyrus Development and Schizophrenia-like Behaviors. Cell Rep. *22*, 456–470. https://doi.org/10.1016/j.celrep.2017.12.044.
17. Matsuoka, R.L., Chivatakarn, O., Badea, T.C., Samuels, I.S., Cahill, H., Katayama, K.I., Kumar, S.R., Suto, F., Chédotal, A., Peachey, N.S., et al. (2011). Class 5 transmembrane semaphorins control selective Mammalian retinal lamination and function. Neuron *71*, 460–473. https://doi.org/10.1016/j.neuron.2011.06.009.
18. Gunn, R.K., Huentelman, M.J., and Brown, R.E. (2011). Are Sema5a mutant mice a good model of autism? A behavioral analysis of sensory systems, emotionality and cognition. Behav. Brain Res. *225*, 142–150. https://doi.org/10.1016/j.bbr.2011.07.008.
19. Goldberg, J.L., Vargas, M.E., Wang, J.T., Mandemakers, W., Oster, S.F., Sretavan, D.W., and Barres, B.A. (2004). An oligodendrocyte lineage-specific semaphorin, Sema5A, inhibits axon growth by retinal ganglion cells. J. Neurosci. *24*, 4989–4999. https://doi.org/10.1523/JNEUROSCI.4390-03.2004.
20. Kantor, D.B., Chivatakarn, O., Peer, K.L., Oster, S.F., Inatani, M., Hansen, M.J., Flanagan, J.G., Yamaguchi, Y., Sretavan, D.W., Giger, R.J., and Kolodkin, A.L. (2004). Semaphorin 5A is a bifunctional axon guidance cue regulated by heparan and chondroitin sulfate proteoglycans. Neuron *44*, 961–975. https://doi.org/10.1016/j.neuron.2004.12.002.
21. Sadanandam, A., Sidhu, S.S., Wullschleger, S., Singh, S., Varney, M.L., Yang, C.S., Ashour, A.E., Batra, S.K., and Singh, R.K. (2012). Secreted semaphorin 5A suppressed pancreatic tumour burden but increased metastasis and endothelial cell proliferation. Br. J. Cancer *107*, 501–507. https://doi.org/10.1038/bjc.2012.298.
22. Chevalier, J., Derkinderen, P., Gomes, P., Thinard, R., Naveilhan, P., Vanden Berghe, P., and Neunlist, M. (2008). Activity-dependent regulation of tyrosine hydroxylase expression in the enteric nervous system. J. Physiol. *586*, 1963–1975. https://doi.org/10.1113/jphysiol.2007.149815.
23. Le Berre-Scoul, C., Chevalier, J., Oleynikova, E., Cossais, F., Talon, S., Neunlist, M., and Boudin, H. (2017). A novel enteric neuron-glia coculture system reveals the role of glia in neuronal development. J. Physiol. *595*, 583–598. https://doi.org/10.1113/JP271989.
24. Ruthazer, E.S., Li, J., and Cline, H.T. (2006). Stabilization of axon branch dynamics by synaptic maturation. J. Neurosci. *26*, 3594–3603. https://doi.org/10.1523/JNEUROSCI.0069-06.2006.
25. Chi, P., Greengard, P., and Ryan, T.A. (2001). Synapsin dispersion and reclustering during synaptic activity. Nat. Neurosci. *4*, 1187–1193. https://doi.org/10.1038/nn756.
26. Chi, P., Greengard, P., and Ryan, T.A. (2003). Synaptic vesicle mobilization is regulated by distinct synapsin I phosphorylation pathways at different frequencies. Neuron *38*, 69–78. https://doi.org/10.1016/s0896-6273(03)00151-x.
27. Greengard, P., Valtorta, F., Czernik, A.J., and Benfenati, F. (1993). Synaptic vesicle phosphoproteins and regulation of synaptic function. Science *259*, 780–785. https://doi.org/10.1126/science.8430330.
28. Caillaud, M., Le Dréan, M.E., De-Guilhem-de-Lataillade, A., Le Berre-Scoul, C., Montnach, J., Nedellec, S., Loussouarn, G., Paillé, V., Neunlist, M., and Boudin, H. (2022). A functional network of highly pure enteric neurons in a dish. Front. Neurosci. *16*, 1062253. https://doi.org/10.3389/fnins.2022.1062253.
29. Jovanovic, J.N., Benfenati, F., Siow, Y.L., Sihra, T.S., Sanghera, J.S., Pelech, S.L., Greengard, P., and Czernik, A.J. (1996). Neurotrophins stimulate phosphorylation of synapsin I by MAP kinase and regulate synapsin I-actin interactions. Proc. Natl. Acad. Sci. USA *93*, 3679–3683. https://doi.org/10.1073/pnas.93.8.3679.
30. Betz, W.J., Mao, F., and Smith, C.B. (1996). Imaging exocytosis and endocytosis. Curr. Opin. Neurobiol. *6*, 365–371. https://doi.org/10.1016/s0959-4388(96)80121-8.
31. Boesmans, W., Gomes, P., Janssens, J., Tack, J., and Vanden Berghe, P. (2008). Brain-derived neurotrophic factor amplifies neurotransmitter responses and promotes synaptic communication in the enteric nervous system. Gut *57*, 314–322. https://doi.org/10.1136/gut.2007.131839.
32. Ho, W.Y., Chang, J.C., Tyan, S.H., Yen, Y.C., Lim, K., Tan, B.S.Y., Ong, J., Tucker-Kellogg, G., Wong, P., Koo, E., and Ling, S.C. (2019). FUS-mediated dysregulation of Sema5a, an autism-related gene, in FUS mice with hippocampus-dependent cognitive deficits. Hum. Mol. Genet. *28*, 3777–3791. https://doi.org/10.1093/hmg/ddz217.
33. Good, P.F., Alapat, D., Hsu, A., Chu, C., Perl, D., Wen, X., Burstein, D.E., and Kohtz, D.S. (2004). A role for semaphorin 3A signaling in the degeneration of hippocampal neurons during Alzheimer's disease. J. Neurochem. *91*, 716–736. https://doi.org/10.1111/j.1471-4159.2004.02766.x.
34. Ko, P.H., Lenka, G., Chen, Y.A., Chuang, E.Y., Tsai, M.H., Sher, Y.P., and Lai, L.C. (2020). Semaphorin 5A suppresses the proliferation and migration of lung adenocarcinoma cells. Int. J. Oncol. *56*, 165–177. https://doi.org/10.3892/ijo.2019.4932.
35. Vieira, J.R., Shah, B., Dupraz, S., Paredes, I., Himmels, P., Schermann, G., Adler, H., Motta, A., Gärtner, L., Navarro-Aragall, A., et al. (2022). Endothelial PlexinD1 signaling instructs spinal cord vascularization and motor neuron development. Neuron *110*, 4074–4089.e6. https://doi.org/10.1016/j.neuron.2022.12.005.
36. Kalil, K., and Dent, E.W. (2014). Branch management: mechanisms of axon branching in the developing vertebrate CNS. Nat. Rev. Neurosci. *15*, 7–18. https://doi.org/10.1038/nrn3650.
37. Li, Z., Hao, M.M., Van den Haute, C., Baekelandt, V., Boesmans, W., and Vanden Berghe, P. (2019). Regional complexity in enteric neuron wiring reflects diversity of motility patterns in the mouse large intestine. Elife *8*. https://doi.org/10.7554/eLife.42669.
38. Skorobogatko, Y., Landicho, A., Chalkley, R.J., Kossenkov, A.V., Gallo, G., and Vosseller, K. (2014). O-linked beta-N-acetylglucosamine (O-GlcNAc) site thr-87 regulates synapsin I localization to synapses and size of the reserve pool of synaptic vesicles. J. Biol. Chem. *289*, 3602–3612. https://doi.org/10.1074/jbc.M113.512814.
39. Gitler, D., Xu, Y., Kao, H.T., Lin, D., Lim, S., Feng, J., Greengard, P., and Augustine, G.J. (2004). Molecular determinants of synapsin targeting to presynaptic terminals. J. Neurosci. *24*, 3711–3720. https://doi.org/10.1523/JNEUROSCI.5225-03.2004.
40. Zhang, M., and Augustine, G.J. (2021). Synapsins and the Synaptic Vesicle Reserve Pool: Floats or Anchors? Cells *10*, 658. https://doi.org/10.3390/cells10030658.
41. Jovanovic, J.N., Sihra, T.S., Nairn, A.C., Hemmings, H.C., Jr., Greengard, P., and Czernik, A.J. (2001). Opposing changes in phosphorylation of specific sites in synapsin I during Ca2+-dependent glutamate release in isolated nerve terminals. J. Neurosci. *21*, 7944–7953. https://doi.org/10.1523/JNEUROSCI.21-20-07944.2001.
42. O'Connor, T.P., Cockburn, K., Wang, W., Tapia, L., Currie, E., and Bamji, S.X. (2009). Semaphorin 5B mediates synapse elimination in hippocampal neurons. Neural Dev. *4*, 18. https://doi.org/10.1186/1749-8104-4-18.
43. Bonnycastle, K., Davenport, E.C., and Cousin, M.A. (2021). Presynaptic dysfunction in neurodevelopmental disorders: Insights from the synaptic vesicle life cycle. J. Neurochem. *157*, 179–207. https://doi.org/10.1111/jnc.15035.
44. Tang, L.T.H., Craig, T.J., and Henley, J.M. (2015). SUMOylation of synapsin Ia maintains synaptic vesicle availability and is reduced in an autism mutation. Nat. Commun. *6*, 7728. https://doi.org/10.1038/ncomms8728.
45. Schemann, M., Sann, H., Schaaf, C., and Mäder, M. (1993). Identification of cholinergic neurons in enteric nervous system by antibodies against choline acetyltransferase. Am. J. Physiol. *265*, G1005–G1009. https://doi.org/10.1152/ajpgi.1993.265.5.G1005.
46. Perkins, K.L. (2006). Cell-attached voltage-clamp and current-clamp recording and stimulation techniques in brain slices. J. Neurosci. Methods *154*, 1–18. https://doi.org/10.1016/j.jneumeth.2006.02.010.

STAR★METHODS

KEY RESOURCES TABLE

REAGENT or RESOURCE	SOURCE	IDENTIFIER
Antibodies		
Rabbit polyclonal anti-Sema5A	Novus Biologicals	Cat: NBP2-20291
Rabbit polyclonal anti-Sema5A	R&D Systems	RRID: AB_10641838; Cat:AF5896
Rabbit polyclonal anti-Plexin A1	Alomone	RRID: AB_2756765; Cat: APR-081
Goat polyclonal anti-Plexin A2	R&D Systems	RRID: AB_10573285; Cat: AF5486
Rabbit monoclonal anti-synapsin 1	Cell Signaling	RRID: AB_2616578; Cat: 5297
Mouse monoclonal anti-β3-tubulin	Sigma-Aldrich	RRID: AB_477590; Cat: T8660
Rabbit polyclonal anti-phospho-synapsin 1(Ser62/67)	Thermo Fisher Scientific	Cat: 11583501
Rabbit polyclonal anti-phospho-synapsin 1 (Ser603)	Thermo Fisher Scientific	RRID: AB_560615; Cat: PA1-4604
Rabbit polyclonal anti-phospho-synapsin 1 (Ser9)	Cell Signaling	Cat: CST2311
Rabbit polyclonal anti-p44/42 MAPK (Erk1/2)	Cell Signaling	RRID: AB_330744; Cat: 9102
Rabbit polyclonal anti-phospho-p44/42 MAPK (Erk1/2) (Thr202/Tyr204)	Cell Signaling	RRID:AB_331646; Cat: 9101
Mouse monoclonal anti-CaMKII alpha	Invitrogen	RRID:AB_325403; Cat: MA1-048
Rabbit monoclonal anti-phospho-CaMKII (Thr286) (D21E4)	Cell Signaling	RRID:AB_2713889; Cat: 12716
Mouse monoclonal anti-β-Actin	Sigma-Aldrich	RRID:AB_476744; Cat: A5441
Mouse monoclonal anti-β3-tubulin (β3-tubulin, clone 6G7)	DSHB	RRID:AB_2393086; Cat: clone 6G7
Mouse monoclonal anti-S100β IgG1	Abnova	Cat: MAB12455
Mouse monoclonal anti-nNOS type I	BD	RRID:AB_397700; Cat: 610308
Rabbit polyclonal anti-ChAT (code PO3, Yeboah)	Gift from Dr M. Schemann[45]	N/A
Rabbit Polyclonal anti-Calbindin D28K	Thermo Fisher Scientific	RRID:AB_2792808; Cat: PA5-85669
Human anti-Hu	Gift from CHU of Nantes[4]	N/A
Goat polyclonal anti-HuC/D (N-15)	Santa cruz Biotechnology, Inc.	RRID:AB_2101223; Cat: sc5977
HRP-conjugated goat polyclonal anti-rabbit IgG (H+L)	Thermo scientific	RRID:AB_228341; Cat: 31460
HRP-conjugated rabbit polyclonal anti-mouse IgG	Sigma-Aldrich	RRID:AB_258431; Cat: A9044
HRP-conjugated donkey polyclonal anti-goat IgG	Bethyl Laboratories, Inc	RRID:AB_66755; Cat: A50-101P
Cy3-conjugated donkey polyclonal anti-mouse IgG (H+L)	Jackson ImmunoResearch	RRID:AB_2315777; Cat: 715-165-151

(*Continued on next page*)

Continued

REAGENT or RESOURCE	SOURCE	IDENTIFIER
Cy3-conjugated donkey polyclonal anti-human IgG (H+L)	Jackson ImmunoResearch	RRID:AB_2340535; Cat: 709-165-149
Cy3-conjugated donkey polyclonal anti-rabbit IgG (H+L)	Jackson ImmunoResearch	RRID:AB_2307443; Cat: 711-165-152
FluoProbes 488 (Cy2) Donkey Anti-Goat IgG (H+L)	Interchim	Cat: FP-SA2110
FluoProbes 488 (Cy2) Donkey Anti-rabbit IgG (H+L)	Interchim	RRID:AB_2686906; Cat: FP-SA5110
AMCA-conjugated Donkey Anti-Mouse IgG (H+L)	Jackson ImmunoResearch	RRID:AB_2340806; Cat: 715-155-150
Chemicals, peptides, and recombinant proteins		
Lipofectamine 2000 reagent	Invitrogen	Cat: 11668027
Recombinant mouse semaphorin 5A-Fc Chimera	R&D systems	Cat: 6584-S5-025
Recombinant Mouse IgG2A FC	R&D systems	Cat: 4460-MG-100
Matrigel Matrix Growth Factor Reduced	Corning	Cat: 356231
Recombinant Rat GDNF, CF	R&D Systems - bio-techne	Cat: 512-GF-010/CF
Collagen type I Rat tail	Corning	Cat: 354236
FM™ 1–43 Dye	Molecular Probes	Cat: T35356
Clarity Western ECL Substrate	Bio-Rad	Cat: 1705061
ProLong Gold Antifade Reagents	ThermoFisher Scientific	Cat: P36930
Critical commercial assays		
QuikChange Lightning Site-Directed Mutagenesis Kit	Agilent Technologies	Cat: 210519
Pierce BCA protein assay Kit	Thermo Fisher Scientific	Cat: 23225
Experimental models: Cell lines		
Green monkey: **COS-7 cells**	ATCC	Cat: CRL-1651; RRID:CVCL_0224
Experimental models: Organisms/strains		
Rats Sprague-Dawley	Janvier Labs, Le Genest Saint-Isle, France	N/A
Recombinant DNA		
pcDNA3.0 -Sema5A-full-length (6xMyc C-terminal-tagged full-length rat Sema5A)	Gift from A. Kolodkin (Johns Hopkins University, Baltimore, USA	N/A
pcDNA3.0 -Sema5A-Fc Rat extracellular domain of Sema5A (amino acid residues 1–961) fused at the C-terminus with a Fc fragment of human IgG (Sema5A-Fc)	Gift from A. Kolodkin (Johns Hopkins University, Baltimore, USA	N/A
pcDNA3.0 -Fc (fragment Fc of human IgG)	Gift from A. Kolodkin (Johns Hopkins University, Baltimore, USA	N/A
pcDNCA3.0 Sema5A-S951C-Fc Rat extracellular domain of Sema5A carrying ASD-associated mutation S951C	This paper	N/A
pcDNCA3.0 Sema5A-S956G-Fc Rat extracellular domain of Sema5A carrying ASD-associated mutation S956G	This paper	N/A
Software and algorithms		
Image Lab software (v6.0.1)	2017, Bio-Rad Laboratories	RRID:SCR_014210
Zen 2 software	Zeiss, Germany	RRID:SCR_013672

(*Continued on next page*)

Continued

REAGENT or RESOURCE	SOURCE	IDENTIFIER
Fiji software	NIH, Open source	RRID:SCR_002285 https://fiji.sc
NIS-Element software	Nikon Instruments Inc	RRID:SCR_014329 https://www.nikoninstruments.com/Products/Software
Easy Electrophysiology (v2.6.3)	Easy Electrophysiology Ltd.	RRID:SCR_021190 https://www.easyelectrophysiology.com/
GraphPad Prism 8	GraphPad Software	RRID:SCR_002798 https://www.graphpad.com/scientific-software/prism/
PATCHMASTER software	HEKA Instrument Inc.	https://www.heka.com/downloads/downloads_main.html#down_patchmaster_next
Other		
Transwell inserts 6.5 mm, 0.4 µm Pore Polyester membrane inserts	Costar	Cat: 3450
Ibidi 24-well plates	ibidi, Gräfelfing, Germany	Cat: 82426

RESOURCE AVAILABILITY

Lead contact

Further information and requests for resources and reagents should be directed to and will be fulfilled by the lead contact, Hélène Boudin (helene.boudin@univ-nantes.fr).

Materials availability

All plasmids generated in this study will be made available upon request by the lead contact.

Data and code availability

- All data reported in this paper will be shared by the lead contact upon request.
- This paper does not report original code.
- Any additional information required to reanalyze the data reported in this paper is available from the lead contact upon request.

EXPERIMENTAL MODEL AND STUDY PARTICIPANT DETAILS

Animals

Pregnant Sprague-Dawley rats were purchased on gestational day 15 (G15) (Janvier Labs, Le Genest Saint-Isle, France). Rats were individually housed in cages on a 12/12-h light/dark cycle with free access to food and water. Mothers and their pups (10–14 pups/litter) were maintained in the same conditions throughout the protocol. At postnatal day 14 (P14), P35 (adolescence), P60 of the progeny, rats were anesthetized with isoflurane (5 min; Abbot) and euthanized by cervical dislocation. For primary cell culture, G15 pregnant rats were anesthetized by isoflurane, euthanized by cervical dislocation and the embryos (E15) were collected to proceed to cell culture. All protocols were carried out in accordance with French standard ethical guidelines for laboratory animals (Agreement # 02476.01).

Cells

Non-human primate (*Green monkey* cell line) COS-7 cells were grown in DMEM (cat: 11965092, Gibco) containing 10% (vol/vol) heat-inactivated FBS (Eurobio), fetal calf serum (FCS), 10 mM glutamine (cat: 25030-024, Gibco), and antibiotics (50,000 IU Penicillin/50,000 IU Streptomycin) (cat: 15140-122,Gibco).

METHOD DETAILS

Western blot

Tissue

Rat distal colon samples collected at P14 and P60 were lysed in 50 mM Tris, 100 mM NaCl, 1% Triton X-100, 1 mM EGTA and protease inhibitors cocktail (cat: 11836153001, cOmplete; Roche, France) solution, pH 7.4, with a tissue homogenizer (Precellys 24, Bertin Technologies,

France) and sonicated three times for 5 sec. For brain samples, used as a positive control for comparison, forebrains of P60 rats were homogenized in RIPA lysis buffer containing protease inhibitor cocktail and centrifuged at 20,000 g for 20 min to collect the supernatant. Protein concentration was quantified using the BCA protein assay (cat: 23225, Thermo Fisher Scientific, Cillebon sur Yvette, France).

Enteric neuron cultures

Cells were gently scraped in 50 µL of RIPA buffer containing protease inhibitor cocktail, 2 mM sodium orthovanadate (cat: S6508, Sigma-Aldrich) and phosphatase inhibitor cocktail 3 (cat: P0044-5ML, Sigma-Aldrich) and were sonicated.

Gut explants

For gut explants cocultured with COS-7 cells, the Matrigel dots containing COS cells were first carefully removed from the culture well and the explants were collected in RIPA buffer and prepared following the procedure described above.

Electrophoresis, transfer, and antibody incubation

Samples were further prepared for electrophoresis by adding the adjusted volume of NuPAGE LDS Sample Buffer 4X (cat: NP0007, Thermo Fisher Scientific) and NuPAGE™ Sample Reducing Agent 10X (cat: NP0009, Thermo Fisher Scientific) and were then heated at 95°C for 5 min and loaded onto a NuPAGE 4–12% Bis-Tris Acrylamide gel (cat: NP0322BOX, Thermo Fisher Scientific) with MES SDS Running Buffer (cat: NP0002, Thermo Fisher Scientific). Loading were 15 µg of proteins for colon and brain tissues and 1/10 of culture well for cell cultures and gut explants. Electrophoretic transfer to nitrocellulose membrane was performed with iBlot Nitrocellulose Transfer stack mini (cat: IB23002, Thermo Fisher Scientific) for 7 minutes at 20 V in an iBlot dry transfer apparatus (cat: IB21001, Thermo Fisher Scientific). Membranes were incubated for 1h in blocking solution composed of Tris-buffered saline (TBS), 0.1% (v/v) Tween-20 and 5% (w/v) non-fat powder milk and were then incubated overnight at 4°C in primary antibodies as follows: rabbit polyclonal anti-Sema5A (respectively, 1:500, cat: NBP2-20291, Novus Biologicals and, 1:200, cat: 4460-MG, R&D Systems), rabbit polyclonal anti-Plexin A1 (1:500, cat: APR-081, Alomone), goat polyclonal anti-Plexin A2 (1:500, cat: AF5486, R&D Systems), rabbit monoclonal anti-synapsin 1 (1:1000, cat: 5297, Cell Signaling), mouse monoclonal anti β-tubulin (1:1000, cat: T8660, Sigma-Aldrich), rabbit polyclonal anti-phospho-synapsin 1 (Ser62/67) (1:1000, cat: 11583501, Thermo Fisher Scientific), rabbit polyclonal anti-phospho-synapsin 1 (Ser603) (1:1000, cat: PA1-4604, Thermo Fisher Scientific), rabbit polyclonal anti-phospho-synapsin 1 (Ser9) (1:1000, cat: CST2311, Cell Signaling), rabbit polyclonal anti-p44/42 MAPK (Erk1/2) (1:1000, cat: 9102, Cell Signaling), rabbit polyclonal anti-phospho-p44/42 MAPK (Erk1/2) (Thr202/Tyr204) (1:1000, cat: 9101, Cell Signaling), mouse monoclonal anti-CaMKII alpha (1:1000, cat: MA1-048, Invitrogen), rabbit monoclonal anti-phospho-CaMKII (Thr286) (D21E4) (1:1000, cat: 12716, Cell Signaling) and mouse monoclonal anti-β-Actin (1:5000, cat: A5441, Sigma-Aldrich). Membranes were washed thoroughly with TBS and incubated for 1h with the appropriate secondary antibody coupled to horseradish peroxidase (HRP) diluted in TBS + 5% non-fat powder milk. Secondary antibodies used are the following: HRP-conjugated goat polyclonal anti-rabbit IgG (H+L) (1:5000, cat: 31460 Thermo scientific), HRP-conjugated rabbit polyclonal anti-mouse IgG (1:5000, cat: A9044 Sigma-Aldrich) and HRP-conjugated donkey polyclonal anti-goat IgG (1:5000, cat: A50-101P, Bethyl). Proteins were detected by chemiluminescence with Clarity Western reagents (cat: 1705061, Bio-Rad) using a ChemiDoc XRS+ system (cat: 1708265, Bio-Rad). The ubiquitous protein β-Actin was revealed and used as reference proteins for loading control and normalizing factor for each deposit. For quantification, the relevant immunoreactive bands were selected and quantified with Image Lab software version 6.0.1 (Bio-Rad). Data are expressed as relative values to β-Actin normalized to the control mean.

Immunofluorescence staining

Tissue

Segments of distal colon from P35 rats were fixed in 0.1 M phosphate-buffered saline (PBS) containing 4% paraformaldehyde (PFA) at room temperature (RT) for 3 h. Whole mounts of longitudinal muscle and myenteric plexus were obtained by microdissection and were permeabilized in 10% BSA, 0.5% Triton X-100 and 0.01% sodium azide diluted in PBS for 2h at RT. Tissues were then incubated with the following primary antibodies: rabbit anti-Sema5A (1:1000, cat: NBP2-20291, Novus Biologicals), mouse anti-β3-tubulin (1:1000, clone 6G7, DSHB), mouse anti-S100β (1:500, cat: MAB12455, Abnova), human anti-Hu[4] (1:5000, gift from the CHU of Nantes, France), rabbit anti-plexin A1 (1:500, cat: APR-081, Alomone labs), goat anti-plexin A2 (1:500, cat: AF5486, R&D systems), mouse anti-nNOS (1:500, cat: 610308, BD), rabbit polyclonal anti-ChAT[45] (1:1000, code PO3, Yeboah, Gift from Dr M. Schemann) and mouse anti-calbindin D28K (1:1000, cat: PA5-85669, Thermo Fisher Scientific) diluted in PBS containing 3% BSA, 0.25% Triton X-100 and 0.01% sodium azide overnight at RT. After two washes with PBS, tissues were incubated for 2h at RT with the appropriate secondary antibodies. Secondary antibodies used are the following: Cy3-conjugated anti-mouse IgG, anti-human IgG, anti-rabbit IgG (1:2000, catalogue numbers, respectively: 715-165-151, 709-165-149, 709-165-149, Jackson ImmunoResearch), FluoProbes 488 (Cy2) Anti-Goat IgG, Anti-rabbit IgG (1:2000, catalogue numbers, respectively: FP-SA2110 and FP-SA5110, Interchim) and, AMCA-conjugated Donkey Anti-Mouse IgG (H+L) (1:2000, cat: 715-155-150, Jackson ImmunoResearch) and mounted with ProLong Gold Antifade Reagents (cat: P36934, ThermoFisher Scientific).

Cell culture and gut explant

ENS, enteric neuron cultures and gut explants were fixed with 4% PFA for 5 min and permeabilized in PBS containing 0.25% Triton X-100 for 5 min. After washings, the samples were incubated in PBS containing 10% BSA for 30 min to block non-specific sites and were then incubated

overnight at RT with primary antibodies diluted in PBS containing 3% BSA and 0.01% sodium azide. Primary antibodies used are the following: rabbit anti-Sema5A (1:500, cat: NBP2-20291, Novus Biologicals), rabbit anti-plexin A1 (1:500, cat: APR-081, Alomone), goat anti-plexin A2 (1:500, cat: AF5486, R&D Systems), goat anti-HuC/D (1:500, cat: sc5977, Santa Cruz Biotechnology), mouse anti-β3-tubulin (1:500, cat: T8660, Sigma-Aldrich) and rabbit anti-synapsin-1 (1:1000, cat: 5297, Cell Signaling). After washings, cells or gut explants were incubated for 2h RT with the appropriate conjugated secondary antibodies diluted in PBS containing 3% BSA and 0.02% azide.

Sholl analyses

For Sholl analyses, pictures of β3-tubulin-labeled axons were acquired with an Axio observer Zeiss microscope using Zen software and a x10 objective. A template of concentric circles distant from 60 and 100 μm from the ganglion center was overlaid on the ganglion using Fiji software. The number of axons crossing each circle was counted for 8 ganglia per culture well. In total, 6 culture wells from 3 experiments were analyzed.

Plasmid constructs

Plasmids encoding rat full-length Sema5A (6xMyc C-terminal-tagged Sema5A), rat extracellular domain of Sema5A (amino acid residues 1–961) fused at the C-terminus with a Fc fragment of human IgG (Sema5A-Fc) and Fc fragment alone as control (Fc) in pcDNA3.0 were provided by A. Kolodkin (Johns Hopkins University, Baltimore, USA). The Sema5A-Fc, corresponding to a soluble protein containing the extracellular domain of Sema5A has previously been shown to be fully functional.[14,19] The Sema5A mutations described in ASD, S951C and S956G,[13] were generated in pcDNA3.0 Sema5A-Fc with the QuikChange Lightning Site-Directed Mutagenesis Kit (210519, Agilent Technologies, les Ulis, France) according to manufacturer's instructions and were verified by sequencing.

Cell cultures

COS-7 cell transfection

COS cells transfections with plasmids encoding Fc or Sema5A constructs were performed using the Lipofectamine 2000 reagent (cat: 11668027, Invitrogen, Cillebon sur Yvette, France). After 1 day of transfection, COS cells were gently scrapped and homogenized in Matrigel Matrix Growth Factor Reduced (cat: 356231, Corning, Darmstadt, Germany) at a concentration of 50,000 cells/μL to subsequently coculture them with ENS cultures and gut explants. For COS cells and enteric neurons cocultures, transfected COS cells were resuspended in enteric glia-conditioned DMEM culture medium (cf. enteric neurons culture section) and plated in Transwell inserts (6.5 mm Transwell ®, 0.4 μm Pore Polyester membrane inserts, cat: 3450, Costar) at a concentration of 64,000 cells/100 μL.

ENS culture

Rat ENS cultures were prepared from E15 rat embryo intestines as previously described.[22] Briefly, intestines were removed and diced into small pieces (1–2 mm length) in Hank's buffered salt solution (HBSS). The tissue fragments were then mechanically triturated with a scalpel and incubated with 0.25% trypsin (cat: T1426, Sigma) for 15 minutes and with 0.1% DNase I (cat: DN25, Sigma) for 10 minutes. The dissociated cells were plated in 24-well plates previously coated with 0.5% gelatin (cat: G6144, Sigma) at a density of 2.4×10^5 cells/cm^2 in DMEM/F12 containing antibiotics and 10% FCS. After 24 h, the medium was replaced with DMEM/F12 containing 1% of N-2 supplement (cat: 17502-048, Life Technologies).

ENS-COS-7 cells coculture

For coculture with Sema5A-Fc-expressing COS cells, 3 μL of transfected COS cells suspended in Matrigel were deposited in the center of the culture well 3h after the plating of gut dissociated cells. To assess the activity of full-length Sema5A on enteric neuron development and allow for cell-cell contact between enteric neurons and COS cells, gut dissociated cells were plated in a culture well containing transfected COS cells (400,000 cells/well). For these two procedures, cells were fixed 3 days after plating. Quantifications in the ENS-COS cell coculture were conducted in the vicinity of the Matrigel dot, within a range covering 0 to 900 μm from the Matrigel's periphery, utilizing the Axio Observer Zeiss microscope and Zen software (Zeiss, Germany), with a x10 objective. The number of Hu-immunoreactive neurons per ganglion in ENS cultures was scored on 20 ganglia from 4 experiments using Axio observer Zeiss microscope.

Gut explants

The intestine of E15 rat embryos was cut into pieces of equal length (1–2 mm) and each piece was placed in a well of a 24-well plate previously coated with collagen type I (cat: 354236, Corning) (0.05 mg/mL in 20 mM acetic acid) in DMEM (cat: 11965092, Gibco) containing 50 ng/ml GDNF, 10% FCS, 2 mM glutamine (cat: 25030-024, Gibco) and antibiotics (cat: 15140-122, Gibco) as previously described.[5] The next day, 3 μL of transfected COS cells suspended in Matrigel (50,000 cells/μl) were placed 5 mm away from the explant. The coculture is maintained for 3 days before fixation for immunostaining or lysis for Western blot. To determine the number and size of synapsin 1 clusters, axonal arborization surrounding gut explants were exhaustively imaged with a x40 objective and the number and size of synapsin 1 clusters were quantified using Fiji software. To define synapsin 1 clusters, a threshold was set to be two times higher than the underlying fluorescence intensity of the axonal processes. The size and number of synapsin 1 clusters were determined using the Fiji particle analysis tool with a cut off particle size of 0.2 μm^2. The number of synapsin 1 clusters was normalized to β3-tubulin area.

Enteric neuron culture

Primary culture of rat enteric neuron was performed as previously described.[28] Briefly, the intestine of E15 rat embryos were cut into pieces of equal length (1–2 mm) and placed in a well of a 24-well culture plate previously coated with collagen type I (cat: 354236, Corning). After 5 days of culture in enteric glia-conditioned neurobasal medium (cat: 21103-049, Gibco) supplemented with B27 (cat: 17504-044-Gibco), 10 mM Glutamine (cat: 25030-024-Gibco), 50,000 IU Penicillin/50,000 IU Streptomycin (cat: 15140-122-Gibco) and GDNF (50 ng/mL) (cat: 512-GF-010/CF R&D Systems - bio-techne), the explants were delicately removed and the cells having migrated out of the explants were detached with Accutase (cat: 07920, StemCell technologies, Saint-Egrève, France). Accutase is then inhibited in DMEM medium, the cells centrifuged (1200rpm, 5 min at RT) and the pellet suspended in enteric glia-conditioned DMEM medium + GDNF (50 ng/mL). Cells were then plated (day 0) either in Ibidi 24-well plates (cat: 82426, ibidi, Gräfelfing, Germany) for FM1-43 imaging or in 24-well plastic culture plates for Western blot analyses. The next day (D1), the antimitotic agent cytosine arabinoside (ARA-C at 5μM) was added to prevent proliferation of glial and muscle cells. Two days after plating (D2), Transwell inserts previously plated with transfected COS cells were placed above enteric neurons that were further incubated for 3 days (to D5). To assess synapsin 1 phosphorylation state in stimulated conditions elicited by K^+-induced depolarization, D5 enteric neurons were stimulated for 60 sec in stimulation buffer (cf. FM1-43) and rested for 15 min in Ca^{2+}-free washing buffer before collection in RIPA lysis buffer.

Sema5A acute treatment on enteric neurons cultures

Enteric neurons culture (at D5) were treated for 5 or 30 min with 4.5 μM of recombinant mouse semaphorin 5A-Fc Chimera (cat: 6584-S5-025, R&D systems) or 4.5 μM recombinant Mouse IgG2A FC (cat: 4460-MG-100, R&D systems) as control. Neurons were lysed in RIPA buffer for Western blot analysis.

FM1-43 imaging

Enteric neurons were incubated for 60 sec at 37°C with 5 μg/mL of FM 1-43 dye (cat: T35356, Molecular Probes) diluted in stimulation buffer composed of 31.5 mM NaCl, 90 mM KCl, 2 mM MgCl2, 2 mM $CaCl_2$, 25 mM HEPES, 30 mM glucose, pH 7.4. Enteric neurons were then washed for 15 min at 37°C in Ca^{2+}-free washing buffer (119 mM NaCl, 2.5 mM KCl, 4 mM $MgCl_2$, 25 mM HEPES, and 30 mM glucose, pH 7.4). Dynamic acquisition was performed using a scanning confocal microscope NIKON A1 RSi (Nikon, Tokyo, Japan) with an oil-immersion objective (×63, NA, 1.40). Preparations were imaged during 4 min in stimulation buffer using Galvano mode at 1 fps (excitation :48nm, emission: 530 ± 20 nm) by NIS-Element software. The fluorescence intensity of FM1-43 clusters was analyzed using the Fiji software. The destaining fraction after 4 min was calculated for each cluster using the formula: 1-(Fluo at 4min/Fluo at 0s).

Patch clamp electrophysiology

Enteric neurons were transferred to a recording chamber and perfused with an external solution containing (in mM): 5 mM Glucose, 2 mM CaCl2, 135 mM NaCl, 5.4 mM KCl, 1 mM MgCl2, 0.33 mM NaH2PO4 and 5 mM HEPES (pH set to 7.4 and osmolarity set to 300 mosmol) at room temperature. Neurons were observed using an Olympus microscope (BX51WIF; Olympus Corporation, Japan) with a X40 water-immersion objective (Olympus U-CAMD3; Olympus Corporation, Japan). Borosilicate pipettes (glass capillaries GC150TF-10, Harvard apparatus, USA) used for recordings were prepared with a micropipette puller (PC-10, Narishige Co, LTD, Japan). Electrodes with a 7–8 mohm resistance, were filled with a 100 mM K-aspartic acid, 6 mM EGTA, 10 mM HEPES, 4.5 mM MgATP, 1 mM $MgCl_2$ and 30 mM KCl solution (pH set to 7.2 and osmolarity set to 300 mosmol). We collected data employing a HEKA amplifier (EPC10 USB double) along with the PATCHMASTER software (HEKA Instrument Inc., New York, USA). The signals underwent digitization at a rate of 1 kHz. Adjustments were made to whole-cell recordings to account for a junction potential of +18 mV. Additionally, the series resistance was continually monitored during the experiment by applying a brief voltage step of −10 mV at the conclusion of each recording session.

Cell-attached

Cell-attached patch-clamp recordings were conducted to observe the spontaneous firing activity of individual enteric neurons while maintaining the cytoplasmic contents. Cell-attached recordings were exclusively conducted in the voltage-clamp mode, ensuring that the injected current was adjusted to 0 pA for a duration of 5 minutes.[46] Firing frequencies (Fi) were calculated by averaging data obtained from 10 consecutive recordings, lasting at least 2 minutes, for each neuron.

Whole-cell patch clamp

Current-clamp

Neurons were subjected to incremental current injections lasting 500ms, starting from a baseline current of −50 pA and gradually increased by 10 pA at a frequency of 0.1 Hz until action potential (AP) firing occurred. Subsequently, we assessed AP parameters after a current injection set at +30 pA above the rheobase. Using Fitmaster (HEKA Elektronik, Germany), we examined the I/V relationship and dynamic membrane properties, including membrane potential, action potential amplitude, action potential frequency, rise and decay time, hyperpolarization amplitude and time taken to reach hyperpolarization amplitude.

Voltage-clamp

Neurons were held at a membrane potential of −60 mV, and miniature post-synaptic currents (mPSCs) were subsequently recorded and analyzed in 250-second recording segments. mPSCs were detected using semi-automated amplitude threshold-based detection "Easy electrophysiology" software.

QUANTIFICATION AND STATISTICAL ANALYSIS

Statistical analysis and data interpretation were conducted using GraphPad Prism 8. Data are presented as mean ± SEM. Group comparisons were executed by first assessing normal distribution and then applying appropriate statistical tests: the t-test or one-way ANOVA for parametric distribution, and the Mann-Whitney test or Kruskal–Wallis test supplemented by Dunn's post-hoc test for nonparametric distribution. Statistical significance thresholds were set as follows: "ns" (non-significant) for p-value >0.05, * for p-value <0.05, ** for p-value <0.01, and *** for $p < 0.001$.